The Effects of the *pep* Nuclear Reaction and Other Improvements in the Nuclear Reaction Rate Library on Simulations of the Classical Nova Outburst

S. Starrfield[1], C. Iliadis[2], W. R. Hix[3], F. X. Timmes[1], W. M. Sparks[4]

ABSTRACT

Nova explosions occur on the white dwarf (WD) component of a Cataclysmic Variable binary stellar system which is accreting matter lost by its companion. When sufficient material has been accreted by the WD, a thermonuclear runaway (TNR) occurs and ejects material in what is observed as a Classical Nova explosion. We have continued our studies of TNRs on $1.25M_{\odot}$ and $1.35M_{\odot}$ WDs (ONeMg composition) under conditions which produce mass ejection and a rapid increase in the emitted light, by examining the effects of changes in the nuclear reaction rates on both the observable features and the nucleosynthesis during the outburst. In order to improve our calculations over previous work, we have incorporated a modern nuclear reaction network into our one-dimensional, fully implicit, hydrodynamic computer code. We find that the updates in the nuclear reaction rate libraries change the amount of ejected mass, peak luminosity, and the resulting nucleosynthesis. Because the evolutionary sequences on the $1.35M_{\odot}$ WD reach higher temperatures, the effects of library changes are more important for this mass. In addition, as a result of our improvements, we discovered that the *pep* reaction ($p + e^- + p \rightarrow d + \nu$) was not included in our previous studies of CN explosions (or to the best of our knowledge those of other investigators). Although the energy production from this reaction is not important in the Sun, the densities in WD envelopes can exceed 10^4 gm cm^{-3} and the presence of this reaction increases the energy generation during the time that the $p - p$ chain is operating. Since it is only the $p - p$ chain that is operating during most of

[1]School of Earth and Space Exploration, Arizona State University, Tempe, AZ 85287-1404:sumner.starrfield@asu.edu; fxt44@mac.com

[2]Department of Physics and Astronomy, University of North Carolina, Chapel Hill, NC27599-3255:

[3]Physics Division, Oak Ridge National Laboratory, Oak Ridge, TN 37831-6354 & Department of Physics and Astronomy, University of Tennessee, Knoxville, TN 37996-1200 :raph@ornl.gov

[4]Science Applications International Corporation, San Diego CA, 92121 & X-4, Los Alamos National Laboratory, Los Alamos, NM, 87545:wms@lanl.gov

the accretion phase prior to the final rise to the TNR, the effect of the increased energy generation is to reduce the evolution time to the peak of the TNR and, thereby, the accreted mass as compared to the evolutionary sequences done without this reaction included. As expected from our previous work, the reduction in accreted mass has important consequences on the characteristics of the resulting TNR and is discussed in this paper.

Subject headings: accretion -binaries: close - cataclysmic variables- classical novae - nuclear astrophysics

1. Introduction

The observable consequences of accretion onto white dwarfs (WDs) in Close Binary stellar systems include the Classical (CN), Symbiotic, and Recurrent Nova (RN) outbursts, and the possible evolution of the Super Soft, Close Binary, X-ray Sources (SSS) to Type Ia Supernovae (SNe Ia) explosions(Starrfield et al. 2004). This diversity of phenomena occurs because of differences in the properties of the secondary star, the mass of the WD, the stage of evolution of the binary system (the luminosity of the WD and the rate of mass accretion onto the WD), and the binary characteristics (orbital separation and mass ratio).

A CN explosion occurs in the accreted hydrogen-rich envelope on the *low-luminosity* WD component of a Cataclysmic Variable (CV) system. Gas is lost by the secondary star and accreted by the WD. One dimensional (1D) hydrodynamic studies, which follow the evolution of the material falling onto the WD from a bare core to the explosion, show that the envelope grows in mass until it reaches a temperature and density at its base that is sufficiently high for ignition of the hydrogen-rich fuel to occur. Both observations of the chemical abundances in CN ejecta and theoretical studies of the consequences of the thermonuclear runaway (TNR) in the WD envelope strongly imply that mixing of the accreted matter with core matter occurs at some time during the evolution to the peak of the explosion. How and when the mixing occurs is not yet known (for discussions, see Gehrz et al. 1998: G1998; Starrfield 2001; Starrfield, Iliadis, and Hix 2008:S2008).

If the bottom of the accreted layer is sufficiently degenerate and well mixed with core material, then a TNR occurs and explosively ejects core plus accreted material in a *fast* CN outburst. The evolution of nuclear burning on the WD, and the total amount of mass that it accretes and ejects depends upon: the mass and luminosity of the underlying WD, the rate of mass accretion onto the WD, the chemical composition in the reacting layers (which includes the metallicity of the CV system), the convective history of the envelope, and the

outburst history of the system.

The *observed* levels of enrichment of elements ranging from carbon to sulfur in CNe ejecta confirm that there is significant dredge-up of matter from the core of the underlying WD which enable CNe to contribute to the chemical enrichment of the ISM. Moreover, extensive studies of CNe with IUE and the resulting abundance determinations reveal the existence of both oxygen-neon-magnesium (ONeMg) WDs and carbon-oxygen (CO) WDs in CN systems (G1998). Therefore, CNe participate in the cycle of Galactic chemical evolution in which dust grains and metal enriched gas in their ejecta, supplementing those of supernovae, AGB stars, and WR stars, are a source of the odd numbered, light and intermediate mass, isotopes (and possibly other elements) in the Interstellar Medium (ISM). Once in the diffuse gas, this material is eventually incorporated into young stars and planetary systems during star formation. CNe are predicted to be the major source of ^{15}N and ^{17}O in the Galaxy and may contribute to the abundances of other isotopes such as ^{7}Li, ^{26}Al and ^{31}P (José and Hernanz 1998; G1998). Theoretical studies predict that the mean mass returned by a CN outburst to the ISM is $\sim 2 \times 10^{-4}$ M$_{\odot}$ (G1998). Using the observationally inferred CN rate of 35±11 per year in our Galaxy (Shafter 1997), it follows that CNe introduce $\sim 7 \times 10^{-3}$ M$_{\odot}$ yr^{-1} of processed matter into the ISM. It is likely, however, that this value is a lower limit (G1998). Recent reviews can be found in G1998, Starrfield (2001), and S2008.

Infrared (IR) observations of the epoch of dust grain formation in the expanding shells of CNe have confirmed that some CNe form amorphous carbon grains, SiC grains, hydrocarbons, and oxygen-rich silicate grains in their ejecta (some CNe form all these in the same outburst), suggesting that a fraction of the pre-solar grains recently identified in meteoritic material (Zinner 1998) may come from CNe (G1998; Amari et al. 2001; José et al. 2004; S2008; but see also Nittler & Hoppe 2005).

Finally, and most important to the studies in this paper, the predictions of the 1D hydrodynamic CN simulations are directly affected by the nuclear reactions that both determine the production of the various isotopes and also produce the energy that drives the ejection of the material and the shape of the light curve. In addition, the temperatures reached around the peak of the TNR sample the regimes of nuclear experiments where the cross sections can be measured directly in the laboratory. Moreover, the rates in the libraries can be tested under the same conditions in which they were measured in the laboratory; no extrapolations are necessary. Therefore, over the years we have used a variety of nuclear reaction rate libraries and determined their influence on the properties of the outburst and the resulting nucleosynthesis. In separate papers we have studied the influence of various nuclear reactions on a subset of the properties of the outburst by post-processing the results of hydrodynamic studies (Parete-Koon, et al. 2003; Hix, et al. 2000, 2003; Iliadis, et

al. 2002). Here, we continue this work by computing a new series of evolutionary sequences with a recent nuclear reaction rate library.

In the next section we briefly describe both the changes to the NOVA code and the four reaction rate libraries that are used for the calculations reported in this paper. In the following section, we report on the results of our new calculations. We continue, in Section 4, with a discussion of the resulting nucleosynthesis, and end with a summary and discussion.

2. The Hydrodynamic Computer Code and Nuclear Reaction Rate Libraries

Over the past few years we have been improving the physics in NOVA and then determining the effects of the improved physics on simulations of the CN outburst (S1998; Starrfield et al. 2000, S2000, S2008). NOVA is a 1D, Lagrangian, fully implicit, hydrodynamic computer code that incorporates a large nuclear reaction rate network. It is described in detail in S1998; S2000; and references therein. As reported in those papers, we have found that improving the opacities, equations-of-state, and the nuclear reaction rate library have had important effects on both the energetics and the nucleosynthesis. Similar results have been reported by the Barcelona group (Hernanz and Josè 2000, and references therein). We have continued to explore the effects of improving the reaction rates used in the calculations on the evolution of the CN outburst. In this paper we compare our earlier studies to new simulations using a reaction rate library of Iliadis which is current as of August 2005 (hereafter I2005). In addition, NOVA is continuously being updated and for the work reported in this paper we have made one major change and numerous minor changes.

The major change is that we no longer use the nuclear reaction network of Weiss and Truran (1990: WT1990) but have switched to the modern nuclear reaction network of Hix and Thielemann (1999: HT1999; see also Parete-Koon et al. 2003). While both networks utilize reaction rates in the common REACLIB format and perform their temporal integration using the Backward Euler method introduced by Arnett and Truran (1969), two important differences are evident. First, WT1990 implemented a single iteration, semi-implicit backward Euler scheme, which had the advantage of a relatively small and predictable number of matrix solutions, but allowed only heuristic checks that the chosen timestep resulted in a stable or accurate solution. In contrast, HT1999 implemented an iterative, fully implicit scheme, repeating the Backward Euler step until convergence is achieved. The iterations provide a measure both of the stability and the accuracy of the solution. Moreover, if convergence does not occur within a reasonable number of iterations, then the timestep is subdivided into smaller intervals until a converged solution can be achieved. Therefore, the fully implicit backward Euler integration can respond to instability or inaccuracy in a way

that is impossible with the semi-implicit backward Euler approach. As a result, the fully iterative approach can often safely employ larger time steps than the semi-implicit approach, obviating the speed advantage of the semi-implicit method's smaller number of matrix solutions per integration step. In addition to the changes in the nuclear reaction network and library, we now use the weak and intermediate screening equations from Graboske et al. (1973) instead of the framework of Salpeter (1954) as described in Cox and Giuli (1968).

Finally, the HT1999 network employs automated linking of reactions in the data set to the species being evolved. This is in contrast to the manual linking employed by WT1990 and many older reaction networks. The automated linking helps to avoid implementation mistakes, as we discovered while performing tests of NOVA in order to understand the source of differences in the results of the simulations between the two versions of the code which used the same reaction rate library but different nuclear reaction networks (plus other differences). We found that while the REACLIB dataset used in prior studies (Politano et al. 1995: P1995; S1998; S2000), included the *pep* reaction ($p + e^- + p \rightarrow d + \nu$: Schatzman 1958; Bahcall & May 1969), it was not linked to abundance changes (or the resulting energy generation) in the WT1990 network. While for Solar modeling energy generation from the *pep* reaction is unimportant (but not the neutrino losses: Rolfs and Rodney 1988), in the WD envelope the density can reach, or exceed, values of 10^4 gm cm^{-3} which, in turn, increases the rate of energy generation over the simulations done without the *pep* reaction included (Starrfield et al. 2007). The increased energy generation reduces the amount of accreted material since the temperature rises faster per gram of accreted material. The effect of changes in the rate of energy generation on simulations of the CN outburst is discussed in detail in S1998. Given a smaller amount of accreted material at the time when the steep temperature rise begins in the TNR, the nuclear burning region is less degenerate and, therefore, the peak temperatures are lower compared to models evolved with the same nuclear reaction rate library used in our previous studies (see the evolution sections below). To the best of our knowledge, none of the previous studies of TNR's in WD envelopes have included this reaction.

Another difference, between this work and our previous studies, is that we do not initiate nuclear burning until the temperatures have reached 9 million degrees in a given mass zone. In our earlier studies, done with the WT network, nuclear burning was initiated at 4 million degrees. We made this change because the reaction rates in the latest libraries are not fit to temperatures below about 10 million degrees and, for temperatures of about 8 million degrees (and lower) some of the rates begin increasing rapidly and unrealistically. Our test runs found that 9 million degrees was a good cut-off value. Fortunately, this has almost no effect on the evolution. We find, for example, that for the sequence done with the Iliadis 2005 reaction rate library at 1.35M$_\odot$, nuclear burning does not start until the sequence has evolved for 7.1×10^3 yr (and the accreted material at that time, $\sim 10^{-6}$M$_\odot$, has reached

down from the surface [mass zone 95] to mass zone 81 [$1.1 \times 10^{-6} M_\odot$]) compared to the total accretion time of 1.8×10^5 yr (where the accreted material [see Table 2] has reached down to mass zone 63 [$2.1 \times 10^{-5} M_\odot$]). Therefore, there is no nuclear burning in the accreted material for only ∼4% of the evolution time and, given that the $p - p$ chain is operating at this time, only a small fraction of the total *nuclear* energy production is neglected.

However, this also means that the outermost mass zones, which have temperatures below 9 million degrees until near the peak of the outburst (when the energy and products of nuclear burning are brought to the surface by convection), do not experience nuclear burning during the accretion phase of the outburst. Therefore, when these layers are mixed into the nuclear burning layers near the peak of the outburst they inject a larger amount of unprocessed nuclei into the TNR than found in our earlier simulations. In order to understand the effects of this difference, we redid the earlier calculations with the older reaction rate libraries (see below).

In this paper we evolve seven different sequences using the same initial conditions but four different reaction rate libraries for each of the two WD masses. We report the results in the tables described in the next section. The first library we use includes the rates from Caughlan and Fowler (1988) and Thielemann et al. (1987, 1988). They were compiled by Thielemann, made available to Truran and Starrfield, and used for the calculations reported in WT1990 and those in Politano et al. (1995: P1995). The first sequence (labeled P1995A), uses the P1995 library, the WT1990 network, and none of the updates listed in the last section. The second sequence (labeled P1995B) uses the latest version of the NOVA code, the HT1999 network, the P1995 library, but the *pep* reaction is not included. A comparison of the results from these two sequences shows the results of updating the code. Most of the differences can be attributed to our use of the Graboske et al. (1973) screening in the latest version.

The third sequence (labeled P1995C) is identical to sequence 2 except that it includes the *pep* reaction and shows how including the *pep* reaction changes the results of the evolution. The next three sequences are done with three different reaction rate libraries. The second library (labeled S1998) uses an updated reaction rate library which contains new rates calculated, measured, and/or compiled by Thielemann and Wiescher. A discussion of the improvements is provided in S1998. The third library (labeled I2001) is described in Iliadis et al. (2001) and was used for the simulations reported in Starrfield et al. (2001). The fourth library (labeled I2005A) is the August 2005 library of Iliadis and the results of calculations done with this library are given in this paper. We label it "This Work" in the plots. These three sequences include the *pep* reaction. Finally, there is one last sequence (labeled I2005B) which is identical to I2005A except that the *pep* reaction is *not* included.

Therefore, we can compare sequences P1995B and P1995C and I2005A and I2005B to determine just the effects of including the *pep* reaction, while sequences P1995C, S1998, I2001, and I2005A show the effects of the different reaction rate libraries on the evolution. In order to prevent confusion, the particular library used for each sequence, the reaction network, and whether or not the *pep* reaction is included are listed in the comments to Tables 2.

References to many of the updated reaction rates used in calculating sequences I2005A and I2005B are given in Table 1 along with some comments on those rates. As required, the ground and isomeric states of ^{26}Al are treated as separate nuclei (Ward & Fowler 1980) and the communication between those states through thermal excitations involving higher lying excited ^{26}Al levels is taken into account. The required γ-ray transition probabilities are adopted from Runkle et al. (2001).

Table 1. Sources of reaction rates[a]

Reaction	Source	Comment
^{8}B(p,γ)^{9}C	Beaumel et al. 2001	in close agreement with Trache et al. 2002
^{11}C(p,γ)^{12}N	Tang et al. 2003	rate of Liu et al. 2003 is higher by a factor of 2
^{13}N(p,γ)^{14}O	Tang et al. 2004	
^{14}N(p,γ)^{15}O	Champagne 2004	based on Runkle et al. 2005
^{15}O(α,γ)^{19}Ne	Davids 2004	
^{17}O(p,γ)^{18}F	Fox et al. 2005	
^{17}O(p,α)^{14}N	Chafa et al. 2005	
^{17}F(p,γ)^{18}Ne	Iliadis et al. 2008	with information from Bardayan et al. 2000
^{18}F(p,γ)^{19}Ne	de Séréville et al. 2005	
^{18}F(p,α)^{15}O	de Séréville et al. 2005	
^{18}Ne(α,p)^{21}Na	Chen et al. 2001	
^{19}Ne(p,γ)^{20}Na	Vancraeynest et al. 1998	
^{23}Na(p,γ)^{24}Mg	Rowland et al. 2004	
^{23}Na(p,α)^{20}Ne	Rowland et al. 2004	
^{25}Al(p,γ)^{26}Si	Iliadis et al. 2008	based on Parpottas et al. 2004 and Bardayan et al. 2002
^{29}Si(p,γ)^{30}P	Iliadis et al. 2008	
^{30}Si(p,γ)^{31}P	Iliadis et al. 2008	

[a]Rates of most other reactions not listed above are adopted from Caughlan & Fowler 1988, Angulo et al. 1999, and Iliadis et al. 2001.

Other changes to NOVA include the use of the analytic fitting formulas of Itoh et al. (1996) for the neutrino energy loss rates from pair ($e^+ + e^- \rightarrow \nu_e + \bar{\nu}_e$), photo ($e^{\pm} + \gamma \rightarrow e^{\pm} + \nu + \bar{\nu}_e$), plasma ($\gamma_{\rm plasmon} \rightarrow \nu_e + \bar{\nu}_e$), bremsstrahlung ($e^- + A^Z \rightarrow e^- + A^Z + \nu_e + \bar{\nu}_e$), and recombination ($e^-_{\rm continuum} \rightarrow e^-_{\rm bound} + \nu_e + \bar{\nu}_e$) processes. As stellar evolution codes generally require derivative information for the Jacobian matrix, our implementation of the Itoh et al. (1996) fitting formulas (available online from cococubed.asu.edu) returns the neutrino loss rate and its first derivatives with respect to temperature, density, $\bar{A}$ (average atomic weight) and $\bar{Z}$ (average charge). Finally, we assume a value of 2 for the mixing-length to scale height ratio (l/H_p). There are additional and numerous small changes to NOVA that had minimal effects on the simulations to be described in the next section.

3. The Initial Conditions and Evolutionary Results

Our initial models are complete $1.25 M_\odot$ and $1.35 M_\odot$ WDs discretized into 95 zones. This is the same number used in our previous studies (P1995, S1998, and S2000). We assume that the material being accreted from the donor star is of Solar (Anders and Grevesse 1989) composition and that it has already mixed with the core material so that the actual accreting composition in this study is 50% Solar and 50% ONeMg material (We use the ONeMg composition of Arnett and Truran 1969.). The use of this composition affects the total amount of accreted mass at the peak of the TNR since it has a higher opacity than if no mixing were assumed (S1998; José et al. 2007). The initial (Solar and ONeMg mixed) abundances by mass are given in column 7 of Table 4.

We use an initial WD luminosity of either $\sim 3 \times 10^{-3}$ $L_\odot$ ($1.25 M_\odot$) or $\sim 4 \times 10^{-3}$ $L_\odot$ ($1.35 M_\odot$). We use a smaller value for the accretion rate (than in S1998), $1.6 \times 10^{-10} M_\odot {\rm yr}^{-1}$, in order to accrete the largest amount of mass possible for a given WD mass. This mass accretion rate is 5 times lower than the lowest rate used in either S1998 or S2000 and was chosen to maximize the amount of accreted material given the increased energy generation from including the *pep* reaction. Studies of accretion onto WDs demonstrate that the results of the evolution depend strongly on the initial WD luminosity and mass accretion rate (c.f., Yaron et al. 2005; G1998; S1998; S2000; S2008, and references therein).

The results of our evolutionary calculations are given in Tables 2 through 5. Tables 2 and 3 give the initial conditions and evolutionary results for both WD masses while Tables 4 and 5 give the abundances of the ejected material (by mass) for the 8 different simulations done with the *pep* reaction included. The numerical factor that multiplies the abundances is given in the first column next to the isotope designation. The rows in Tables 2 and 3 are the reaction rate library, the accretion time to the TNR ($\tau_{\rm acc}$), the accreted mass ($M_{\rm acc}$), peak

temperature in the TNR (T_{peak}), peak rate of energy generation during the TNR ($\epsilon_{\rm nuc-peak}$), peak luminosity ($L_{\rm peak}$), peak effective temperature ($T_{\rm eff-peak}$), ejected mass ($M_{\rm ej}$), and the peak expansion velocity after the radii of the surface layers have reached $\sim 10^{13}$cm ($V_{\rm max}$). By this time the outer layers are optically thin, have far exceeded the escape velocity at this radius, and there is no doubt that they are escaping.

As mentioned in the last section, the first three sequences (P1995A, P1995B, and P1995C) employ the P1995 reaction rate library. As shown in Tables 2 and 3, the three different sequences using the P1995 library provide a clear picture both of the impact of the *pep* reaction as well as the other updates to the NOVA code. Since neither sequence P1995A nor P1995B included the *pep* reaction, the differences between these two sequences shows only the impact of the updates to the NOVA code, which are noticeable but generally small. Most of these differences can be attributed to our use of the Graboske et al. (1973) weak and intermediate screening in this paper and not in earlier papers.

In contrast, much larger differences are seen when sequence P1995B is compared to P1995C which does include the *pep* reaction but is otherwise identical. This conclusion is reinforced by comparing sequences I2005A and I2005B (both calculated with the latest library [I2005] and current version of NOVA) since I2005A includes the *pep* reaction and it is not included in I2005B. Tables 2 ($1.25M_\odot$) and 3 ($1.35M_\odot$) show that for both WD masses the largest change in the results of the evolution occurs with the inclusion of the *pep* reaction. If we compare rows P1995B and P1995C or rows I2005A or I2005B, then the increase in energy production from adding the *pep* reaction to the network results in a significant decrease in both accretion time and accreted mass. Because there is less accreted mass on the WD at the time of the TNR, all the peak values are smaller. However, the effects are much more important for the $1.35M_\odot$ evolution than for the $1.25M_\odot$ evolution. This is because the density is higher in the more massive WD at the beginning of the TNR and, therefore, the *pep* reaction provides more energy ($\epsilon \sim \rho^2$). Interestingly enough, the peak temperatures reached in the two $1.35M_\odot$ simulations without the *pep* reaction (P1995B and I2005B) exceed 5×10^8K which is sufficiently high for CNO breakout (the $^{14}O(\alpha,\gamma)$ and $^{15}O(\alpha,\gamma)$ reactions) to occur (see below). Unfortunately, evolution without the necessary physics of the *pep* reaction included is not realistic and we will have to look elsewhere for initial conditions that produce sufficiently high temperatures for breakout.

If we compare the results for the four sequences with the *pep* reaction included (P1995C, S1998, I2001, I2005A), we see that changes in the nuclear reaction rate library produce differences in ejected mass and peak luminosity for both the $1.25M_\odot$ and $1.35M_\odot$ evolutionary sequences. The results of the evolutionary sequences show that because the WD mass is larger and the radius is smaller for $1.35M_\odot$, the mass zones where the TNR occurs reach

higher densities and higher peak temperatures than do the sequences at lower WD mass (Starrfield 1989; S2008; Yaron et al. 2005). At $1.35M_{\odot}$ the sequence done with the latest reaction rate library (I2005A) accretes and ejects the lowest amount of mass moving at the lowest ejection velocities. In addition, the peak luminosity and effective temperature is lowest for the calculation done with this library. The amount of ejected mass and the ejection velocities are in disagreement with the observations (S2008).

Table 2 shows that only about 25% of the accreted material is ejected in the explosive phase of the outburst at $1.25M_{\odot}$ and Table 3 shows about 60% of the accreted material is ejected at $1.35M_{\odot}$. This is a common feature of our 1D hydrodynamic simulations (G1998; S2008). The material that is not ejected returns to quasistatic equilibrium on the WD and stays luminous and hot with radii exceeding 10^9cm. X-ray studies of this phase of evolution for a CN in outburst indicate that we are observing a hot, luminous stellar atmosphere (Petz et al. 2005; Ness et al. 2007) just as in the Super Soft X-ray Binaries such as CAL 83 (Kahabka & van den Heuvel 1997; Lanz et al. 2005). The predicted time required to burn the remaining envelope material and return the CN to quiescence can exceed 100 yr (Starrfield 1989) which is not observed (Orio 2004). It has been proposed that the remaining material is ejected via radiation pressure driven mass loss on short timescales (Starrfield 1979; MacDonald, Truran, and Fujimoto 1985; Starrfield et al. 1991). Nevertheless, some of the accreted envelope may actually be burnt to helium enriched material and become part of the material ejected in the next CN outburst (Krautter et al. 1996). However, the amount of accreted material that is not ejected suggests that it is insufficient to counteract the amount of WD core mass lost in the outburst. As a result, the WD is losing mass as a result of the CN outburst and CNe cannot be the progenitors of Supernovae of Type Ia.

Figure 1 shows the variation of temperature with time for the zone where peak conditions in the TNR occur in the $1.25M_{\odot}$ evolutionary sequences. In this figure and all other figures we plot only the four simulations done with the *pep* reaction included. The specific evolutionary sequence is identified on the plot and in the caption. The reference to the nuclear reaction rate library used for that calculation is given in the caption for Figure 1 and indicated on the figure. The designation "This Work" refers to the I2005A sequence as described in the tables and discussed earlier. The time coordinate is chosen to clearly show the rise and decline time of each evolutionary sequence. Interestingly enough, the rise time and peak temperature are nearly the same for all four sequences at $1.25M_{\odot}$.

Figure 2 shows the same plot for the sequences at $1.35M_{\odot}$. Here we see differences between the four simulations. Peak temperature drops from about 413 million degrees to 392 million degrees and peak nuclear energy generation drops by about a factor of 2 from the oldest library to the newest library (8.4×10^{17}erg gm^{-1}s^{-1} to 4.4×10^{17}erg gm^{-1}s^{-1}).

The temperature declines more rapidly for the sequence (P1995C) computed with the oldest reaction library (P1995) because there was a larger release of nuclear energy throughout the evolution so that the overlying zones expanded more rapidly and the nuclear burning region cooled more rapidly than in the other sequences. In contrast, the newest library, showing the smallest expansion velocities, cools slowly. There is a factor of two difference in the time coordinate used for Figures 1 and 2 because the simulations at $1.35M_{\odot}$ evolve much more rapidly near the peak of the TNR than those at $1.25M_{\odot}$. This is a direct result of the higher gravity and higher degeneracy in the nuclear burning region of the more massive WDs.

The evolution of the total nuclear energy generation in the nuclear burning layers (in Solar units: $L/L_{\odot}$) as a function of time for each mass is shown in Figures 3 ($1.25M_{\odot}$) and 4 ($1.35M_{\odot}$). The time coordinates are the same as those used in Figures 1 and 2, respectively. Again, there is hardly any difference at the lower WD mass but at $1.35M_{\odot}$ the peak for the calculation done with the latest library is definitely lower than seen in the earlier libraries.

Figures 5 and 6 show the variation of the effective temperature ($T_{\rm eff}$) with time as the layers begin their expansion. We plot the results with the same time coordinates as in Figures 1 and 2 and these plots show how rapidly the energy and β^+-unstable nuclei reach and heat the surface layers. Note that peak $T_{\rm eff}$ occurs when the WD radius is still small and earlier in the evolution than when peak luminosity occurs. The large amplitude oscillations seen in the sequences using the older libraries, and not in that from the latest library, are caused by the intense and rapid heating of the surface layers. They expand, cool, collapse back onto the surface, and expand again. The outer layers are still deep within the gravitational potential well of the WD (since hardly any expansion has occurred at the time of the oscillations) and so the "quasi"-period is that of the free-fall time for the underlying WD. After a few seconds the outer layers are expanding sufficiently rapidly, have cooled, and the oscillations cease. They are not present in the sequence using the latest library because surface heating is less important. The outburst evolves more gradually and the star has started to expand by the time that the β^+-unstable nuclei reach the surface. This can also be seen in Figure 7 ($1.35M_{\odot}$) which shows the velocity of the surface layers as a function of time around the time of peak temperature in the nuclear burning region.

Figures 8 and 9 show the variation with time of the surface luminosity (for the first 11 hours of the TNR) for each of the two WD masses. The intense heat from the β^+-unstable nuclei causes the luminosity to become super-Eddington and the layers begin expanding. However, they are still deep within the potential well of the WD and oscillate for a few seconds. In contrast, the sequence done with the latest library does not become as luminous and the initial oscillations exhibit a much smaller amplitude. These figures imply that if we could observe a CN sufficiently early in the outburst, then it would be super-Eddington and

emitting soft X-rays. However, by the time a CN is typically discovered its luminosity has declined to below Eddington. In contrast to this result, however, the IUE observations of LMC 1991 showed that it was super-Eddington for more than 10 days (Schwarz et al. 2001) a result that is not predicted by any existing CN simulations (S2008).

The initial spike (at a time of about 100 s) is caused by a slowing of the expansion as the energy produced by the β^+-decays decreases. After this time, expansion and cooling of the outer layers causes the opacity to increase and radiation pressure then accelerates the layers outward. The continuous flow of heat from the interior, combined with the increase in opacity, causes another increase in luminosity until the peak is reached.

4. Nucleosynthesis

In this section we present the predicted ejecta abundances for the four sequences at each WD mass done with the *pep* reaction included. Because it is a necessary piece of the $p-p$ reaction chain, calculations done without it included in the reaction network are not realistic and we do not report the abundance results for the three sequences done without the *pep* reaction at each WD mass. However, we do provide two plots which show the effects on the abundances of not including the *pep* reaction and discuss them below. The results for each nucleus in our nuclear reaction network are given as mass fraction in Table 4 ($1.25M_\odot$) and Table 5 ($1.35M_\odot$). The factor multiplying each isotope can be found just to the right of the isotopic designation. Note that the right hand column in Table 4 is the initial abundance of the given nucleus (we do not repeat this column in Table 5).

In order to more clearly show which nuclei are produced by CNe explosions, in Figures 10 and 11 we plot the stable, ejected nuclei divided by the Anders and Grevesse (1989) Solar abundances. In both figures the x-axis is the atomic mass number. The y-axis is the logarithmic ratio of the ejecta abundance divided by the Solar abundance of the same nucleus. The most abundant isotope of a given element is marked by an asterisk and isotopes of the same element are connected by solid lines and labelled by the given element. These plots are patterned after similar plots in Timmes et al. (1995). They show for both WD masses that we predict that ^{15}N, ^{17}O, and ^{31}P are overproduced by a factor of 10^4 in CNe ejecta. There are other nuclei that are overproduced by factors of a thousand and could be important for CN nucleosynthesis. In Figures 12 ($1.25M_\odot$) and 13 ($1.35M_\odot$) we show the ratio of the ejected abundances for the simulation (I2005A) done with the *pep* reaction (using the I2005 reaction rate library) compared to a simulation (I2005B) done without the *pep* reaction (also using the I2005 library). The plot style is the same as for Figures 10 and 11 as described above except that the y-axis is *linear* and not logarithmic.

The initial abundance of ^{1}H is 0.365. (This value is half the solar abundance of Anders and Grevesse [1989].) The hydrogen abundance in the ejected gases for the 1.25$M_{\odot}$ I2005A sequence has declined to ∼0.31. This decline of ∼0.05 in mass fraction results in a total energy production from proton captures of $\sim 4 \times 10^{46}$ erg which agrees with the values typically quoted for observed CN explosions (Starrfield 1989; G1998; S2008). Interestingly, the ejecta abundance of ^{4}He decreases slightly as the reaction rate library is improved and the smallest increase occurs in the calculations done with the two most recent libraries. A ^{4}He ejecta abundance of 0.16 is far smaller than the values typically quoted for observed CN ejecta (G1998 and references therein). We, therefore, support the speculation of Krautter et al. (1996; see also S1998 and S2000) that the large amount of helium observed in CN ejecta implies: (1) that most of the ejected helium was mixed up from the outer layers of the WD by the TNR; and (2) that it was actually produced in previous CN outbursts and subsequent nuclear burning on the WD.

Turning to the more massive nuclei, the abundances of ^{12}C and ^{13}C drop by about a factor of two from the oldest to the newest reaction rate libraries while ^{14}N increases by about a factor of two and ^{15}N declines by slightly less than a factor of two. Note that the abundance of ^{15}N far exceeds that of ^{14}N and it is likely that the nitrogen observed in CN ejecta is mostly ^{15}N rather than ^{14}N. Therefore, our speculation about helium may also hold true for nitrogen. The observed nitrogen is probably ^{15}N produced in previous outbursts, mixed into the newly accreted material, and then ejected during the current CN outburst.

Similarly, ^{16}O declines by about 30% while ^{17}O increases by more than a factor of two. In fact, ^{17}O is the most abundant of the CNO nuclei in the ejecta and the abundances of ^{15}N and ^{17}O exceed those of the even-numbered isotopes. Finally, the C/O ratio in the ejecta drops from about 30% to about 8% from the earliest to the latest library. Other interesting nuclei at this WD mass are ^{18}O which drops about a factor of 10 as the library is improved, ^{22}Na whose abundance remains virtually unchanged as the library is improved, ^{24}Mg which drops a factor of 3 and is severely depleted from its initial abundance, and both ^{26}Al and ^{27}Al which drop by about a factor of two in abundance.

We also find that most of the higher mass nuclei (^{40}Ca is the most massive nucleus in our network), are all produced by the TNR in the outburst (see Table 4). Interestingly, the abundances of ^{28}Si, ^{29}Si, and ^{30}Si are largest in the calculations done with the latest library while the abundances of ^{33}S, ^{34}S, and ^{35}Cl decrease in the latest library. Finally, ^{36}Ar is depleted by the outburst (its final abundance is less than the initial abundance) in all sequences except P1995C.

The ejecta abundance results for TNRs on 1.35$M_{\odot}$ WDs are given in Table 5 for the same reaction rate libraries used in the study at lower WD mass. Hydrogen is depleted

by a larger amount at this WD mass than for the $1.25M_{\odot}$ sequences resulting in a total energy production from proton captures of $\sim 3 \times 10^{46}$ erg. This value is smaller than in the lower mass sequence because the $1.35M_{\odot}$ sequences accrete less mass. As in the sequences at $1.25M_{\odot}$, the helium abundance in the ejecta is small compared to the observed helium abundances in CN ejecta and the results at this WD mass also support our prediction that the accreted material mixed with the outer layers of the WD at some time during the outburst. We emphasize, in addition, that the large helium abundances observed in recurrent novae such as U Sco or V394 CrA imply that mixing with the WD has occurred in these systems even if the total CNO abundances in their ejecta are not dramatically enriched over solar (Shore et al. 1991).

Examining the behavior of the individual abundances, we see that ^{12}C and ^{13}C are virtually unchanged by the updated reaction rates. In contrast, the abundance of ^{14}N nearly doubles and that of ^{15}N decreases by a factor of two going from the earliest to the latest reaction rate library. ^{16}O doubles in abundance while ^{17}O grows by a factor of 60 and becomes the most abundant of the CNO nuclei in the ejecta. For this WD mass and the latest library, the C/O ratio is 0.12. The abundance of ^{18}O declines by nearly a factor of 5 and the abundances of ^{18}F and ^{19}F also decline by large factors in the sequence done with the latest library.

The initial abundance of ^{20}Ne in all four sequences is 0.25 (see Table 4) so that it is depleted by a smaller amount in the calculations done with the latest library. The abundance of ^{22}Na decreases with the library update and ^{24}Mg is severely depleted by the TNR. In fact, all the Mg isotopes are depleted in the calculations done with the latest library. In contrast, the ejecta abundance of ^{26}Al is unchanged by the changes in the reaction rates while the abundance of ^{27}Al drops by a factor of two. We also find, contrary to a conclusion in Politano et al. (1995), that the amount of ^{26}Al ejected is virtually independent of WD mass.

All the Si isotopes (^{28}Si, ^{29}Si, and ^{30}Si) are enriched in the calculations done with the latest library and ^{29}Si, and ^{30}Si are more abundant in the $1.35M_{\odot}$ simulations than the $1.25M_{\odot}$ simulations. Other nuclei whose abundances are largest in the calculations done with the latest library are ^{31}P and ^{32}S. These nuclei are also more abundant at the higher WD mass. In addition, while the ejecta abundance of ^{33}S does not depend on the reaction rate library, it is nearly 30 times more abundant in the calculations done with the more massive WD. Finally, we note that while the ejecta abundances of ^{34}S, ^{35}Cl, ^{36}Ar, and ^{40}Ca have all declined as the reaction rate library has been improved, we predict that they will be produced in a nova TNR since their final abundances exceed the initial abundances.

The effects of including the *pep* reaction on ejecta abundances are shown in Figures 12 and 13 in which we plot the ratio of the ejecta abundance of the sequence with the

pep reaction included divided by the abundance from the equivalent sequence with the *pep* reaction not included. Figure 12 shows that most nuclei have a higher abundance in the $1.25M_\odot$ sequence with no *pep*. This is also true for the $1.35M_\odot$ WD sequence with the notable exception of the carbon isotopes, ^{14}N, ^{20}Ne, ^{21}Ne, and ^{32}S. These results are as expected since the sequence at $1.35M_\odot$ reaches to higher temperatures.

Finally, given the high temperatures attained in the $1.35M_\odot$ sequence without the *pep* reaction included, we checked to determine if breakout had occurred. We found that the total CNO abundances decreased from their initial values in both sequences (using the latest reaction library only). As expected, the sequence done without the *pep* reaction showed the most depletion but for neither mass was it sufficiently large to be observable.

5. Summary and Discussion

In this paper we examined the consequences of improving the nuclear reaction rate library on our simulations of TNRs on $1.25M_\odot$ and $1.35M_\odot$ ONeMg WDs. We found that the changes in the rates affected predictions of both the nucleosynthesis and the observable features of the evolution such as peak luminosity, peak effective temperature, ejected mass, and ejecta velocities. A major change to our previous calculations, that effects virtually all features of the predicted outburst, has been the inclusion of the *pep* reaction in the $p-p$ chain. This reaction is important during the accretion phase of the evolution because the density of the accreting material quickly reaches values of $\sim 10^4$ gm cm^{-3}. This high a density increases the nuclear energy generation over studies done with the *pep* reaction absent. The increased energy generation reduces the time to reach the TNR and, thereby, the amount of accreted material and as a result the peak values of temperature and energy generation are smaller than we have found in our previous studies.

If we examine the abundance predictions for the four $1.25M_\odot$ sequences done with the *pep* reaction included, we see that the differences caused by improving the reaction rate library are that the abundance of ^{12}C declines by about a factor of two (all abundances are given in mass fraction), ^{14}N increases by almost a factor of two, and ^{16}O declines by about a factor of 1.5. Both ^{12}C and ^{13}C are depleted in the latest sequence (compared to the P1995 library) as is ^{15}N while ^{17}O is enriched in the calculation done with the latest reaction rate library. In addition, in all four sequences the ejected oxygen exceeds carbon as found in our earlier studies. This result continues to be puzzling in light of the production of carbon rich dust grains in CN ejecta (G1998). It is possible that the carbon dust grain forming CNe occur on lower mass CO WDs which never develop sufficiently hot nuclear burning temperatures to deplete the carbon as compared to oxygen. As we examine the

more massive nuclei at $1.25M_{\odot}$, we see that ^{26}Al, and ^{27}Al are depleted in the simulations done with the latest library while ^{32}S is enhanced. Interestingly, the abundance of ^{22}Na increased with the sequences done with the libraries intermediate in time but then decreased to a value nearly equal to that in the earliest library.

The effects of changing the nuclear reaction library are also apparent for the sequences at $1.35M_{\odot}$. Both ^{12}C and ^{13}C drop in abundance while ^{14}N, ^{16}O and ^{17}O increase in abundance. We find that while the ejecta abundance of ^{22}Na is lowest in simulations done with the I2005 library, it is still a factor of about 5 more abundant at $1.35M_{\odot}$ than at $1.25M_{\odot}$. The abundance of ^{26}Al is unchanged while that of ^{27}Al declined by about a factor of 2. In addition, the abundance of ^{26}Al is roughly constant from one WD mass to the other while the abundance of ^{22}Na declined by about a factor of 2 as the WD mass increased. This is not what we reported in earlier studies (done without the *pep* reaction) using older libraries where we found that the abundance of ^{26}Al declined as the WD mass increased. Finally, we note that the abundance of ^{32}S is largest for the latest library at $1.35M_{\odot}$. In fact, it reaches 4% of the ejected material.

In summary, the nucleosynthesis predictions from our simulations show significant impact from improvements in the reaction rates over the past 15 or so years. Observable features of the models, such as the variation of the effective temperature and luminosity with time, and also the mass ejected, exhibit a notable influence from changes in these rates, because of their dependence on heating from the decays of nucleosynthesis products that have been mixed into the outer layers.

We thank L. Bildsten, A. Champagne, R. Gehrz, J. Krautter, H. Schatz, D. Townsley, J. Truran, and C. E. Woodward for interesting discussions. We are grateful to the anonymous referee whose comments improved the presentation of this paper. SS thanks J. Aufdenberg and ORNL for generous allotments of computer time. CI is supported in part by the U.S. Department of Energy under Contract No. DE-FG02-97ER41041. WRH has been partly supported by the National Science Foundation under contracts PHY-0244783 and AST-0653376. Oak Ridge National Laboratory is managed by UT-Battelle, LLC, for the U.S. Department of Energy under contract DE-AC05-00OR22725. S. Starrfield acknowledges partial support from NSF and NASA grants to ASU.

Table 2. Initial Parameters and Evolutionary Results for $1.25M_{\odot}$ White Dwarfs [a]

Sequence:	P1995A[b]	P1995B[c]	P1995C[d]	S1998[e]	I2001[f]	I2005A[g]	I2005B[h]
$\tau_{\rm acc}(10^5$ yr)	5.2	5.0	3.8	3.8	3.8	3.8	5.0
$M_{\rm acc}(10^{-5}M_{\odot})$	8.2	8.0	6.0	6.0	6.1	6.1	8.0
$T_{\rm peak}(10^6{\rm K})$	348	347	321	321	320	320	347
$\epsilon_{\rm nuc-peak}(10^{17}{\rm erg\ gm^{-1}s^{-1}})$	2.8	2.7	2.0	2.1	1.3	1.3	1.8
$L_{\rm peak}$ $(10^5L_{\odot})$	4.2	5.7	2.6	2.3	2.0	2.6	5.7
$T_{\rm eff-peak}(10^5{\rm K})$	9.1	9.4	8.3	8.6	6.5	6.6	9.4
$M_{\rm ej}(10^{-5}M_{\odot})$	5.0	4.8	1.8	1.5	.7	1.5	3.3
$V_{\rm max}({\rm km\ s^{-1}})$	3563	3681	3081	2860	2772	3143	3761

[a]The initial model for all evolutionary sequences had $M_{\rm WD}$=1.25$M_{\odot}$, $L_{\rm WD}=3.2\times10^{-3}L_{\odot}$, $T_{\rm eff}=1.9\times10^4$K, $R_{\rm WD}$=3497 km, and a central temperature of 1.2×10^7K

[b]Politano et al. (1995) library: pep reaction *not* included (Weiss and Truran [1990] network); Anders and Grevesse (1989) Solar abundances

[c]Politano et al. (1995) library: pep reaction *not* included (Hix & Thielemann [1999] network); Anders and Grevesse (1989) Solar abundances

[d]Politano et al. (1995) library: pep reaction included (Hix & Thielemann [1999] network); Anders and Grevesse (1989) Solar abundances

[e]Starrfield et al. (1998) library: pep reaction included (Hix & Thielemann [1999] network); Anders and Grevesse (1989) Solar abundances

[f]Iliadis et al. (2001) library: pep reaction included (Hix & Thielemann [1999] network); Anders and Grevesse (1989) Solar abundances

[g]Iliadis 2005 library (this work): pep reaction included (Hix & Thielemann [1999] network); Anders and Grevesse (1989) Solar abundances

[h]Iliadis 2005 library (this work): pep reaction *not* included (Hix & Thielemann [1999] network); Anders and Grevesse (1989) Solar abundances

Table 3. Initial Parameters and Evolutionary Results for $1.35M_{\odot}$ White Dwarfs [a]

Reaction Library:	P1995A	P1995B	P1995C	S1998	I2001	I2005A	I2005B
$\tau_{\rm acc}(10^5$ yr)	2.5	3.6	2.1	2.1	2.1	1.8	3.8
$M_{\rm acc}(10^{-5}M_{\odot})$	3.9	5.8	3.3	3.3	3.3	2.8	6.1
$T_{\rm peak}(10^6{\rm K})$	459	524	413	414	407	392	519
$\epsilon_{\rm nuc-peak}(10^{17}{\rm erg\ gm^{-1}s^{-1}})$	22.8	48.6	8.4	8.6	4.9	4.4	21.8
$L_{\rm peak}$ $(10^5L_{\odot})$	8.0	13.4	9.6	8.0	7.3	5.9	10.9
$T_{\rm eff-peak}(10^5{\rm K})$	20.0	21.4	13	13	8.8	8.8	18.1
$M_{\rm ej}(10^{-5}M_{\odot})$	3.3	4.1	2.3	2.3	2.3	1.7	4.3
$V_{\rm max}({\rm km\ s^{-1}})$	6050	7452	5239	4755	4787	4513	6599

[a]The initial model for all evolutionary sequences had $M_{\rm WD}=1.35M_{\odot}$, $L_{\rm WD}=4.2\times10^{-3}L_{\odot}$, $T_{\rm eff}=2.5\times10^4$K, $R_{\rm WD}=2495$ km, and central temperature of 1.2×10^7K

Table 4. Comparison of the Ejecta Abundances for $1.25M_{\odot}$ White Dwarfs[a]

Sequence:	P1995C	S1998	I2001	I2005A	Init.Abund.[b]
H	0.30	0.30	0.31	0.31	0.365
^{3}He($\times10^{-10}$)	6.8	6.2	9.8	6.8	58000
^{4}He	0.18	0.17	0.16	0.16	0.133
^{7}Li($\times10^{-8}$)	6.5	.94	22.	14.	0.0
^{7}Be($\times10^{-8}$)	2.1	7.6	1.2	0.5	0.0
^{12}C($\times10^{-3}$)	8.0	8.6	2.5	4.4	0.94
^{13}C($\times10^{-3}$)	5.6	7.7	1.6	2.6	0.012
^{14}N($\times10^{-3}$)	5.4	7.4	4.8	9.6	0.0023
^{15}N($\times10^{-2}$)	7.5	7.5	4.1	4.6	9.1×10^{-5}
^{16}O($\times10^{-3}$)	13.	12.	8.5	9.4	150
^{17}O($\times10^{-2}$)	3.3	3.0	9.4	7.7	8.5×10^{-5}
^{18}O($\times10^{-3}$)	3.3	1.9	0.4	0.2	0.0048
^{18}F($\times10^{-4}$)	6.9	10.	1.5	0.7	0.0
^{19}F($\times10^{-5}$)	5.9	4.8	0.8	0.3	0.011
^{20}Ne	0.21	0.21	0.20	0.21	0.25
^{21}Ne($\times10^{-5}$)	8.4	8.4	6.4	10.	0.09
^{22}Ne($\times10^{-6}$)	1.1	0.9	1.0	0.2	28.
^{22}Na($\times10^{-3}$)	4.8	7.3	6.8	4.5	0.0
^{23}Na($\times10^{-2}$)	2.1	1.5	2.3	1.9	9.2×10^{-4}
^{24}Mg($\times10^{-4}$)	9.0	2.5	3.2	2.8	1000
^{25}Mg($\times10^{-2}$)	3.3	0.9	1.2	1.2	1.9×10^{-3}
^{26}Mg($\times10^{-4}$)	43.	19.	6.1	6.6	0.22
^{26}Al($\times10^{-3}$)	5.2	1.9	1.7	2.1	0.0
^{27}Al($\times10^{-2}$)	1.9	1.9	1.0	1.0	0.0016
^{28}Si($\times10^{-2}$)	3.6	5.9	5.0	5.5	0.018
^{29}Si($\times10^{-3}$)	4.8	5.4	12.	10.	9.5×10^{-3}
^{30}Si($\times10^{-2}$)	1.6	2.2	2.5	3.3	6.5×10^{-4}
^{31}P($\times10^{-2}$)	1.0	1.4	1.9	1.6	2.3×10^{-4}
^{32}S($\times10^{-2}$)	0.6	1.1	1.5	1.3	0.011
^{33}S($\times10^{-5}$)	43.	4.4	8.0	7.0	0.09
^{34}S($\times10^{-5}$)	8.3	1.4	2.8	1.2	0.5

Table 4—Continued

Sequence:	P1995C	S1998	I2001	I2005A	Init.Abund.[b]
^{35}Cl($\times 10^{-5}$)	2.3	0.7	1.4	0.6	0.098
^{36}Ar($\times 10^{-5}$)	2.6	0.4	0.3	0.2	1.9
^{40}Ca($\times 10^{-5}$)	1.7	1.7	1.7	1.7	1.7

[a]All abundances are Mass Fraction and are to be multiplied by the number following the isotopic designation

[b]Initial Abundances: half Solar (Anders & Grevesse 1989) and half ONeMg

Table 5. Comparison of the Ejecta Abundances for 1.35$M_\odot$ White Dwarfs[a]

Sequence:	P1995C	S1998	I2001	I2005A
H	0.27	0.27	0.27	0.28
^{3}He ($\times10^{-10}$)	2.3	2.1	2.1	1.8
^{4}He	0.18	0.18	0.17	0.17
^{7}Li ($\times10^{-7}$)	2.2	1.2	2.2	1.9
^{7}Be ($\times10^{-8}$)	0.0	9.8	4.1	1.4
^{12}C ($\times10^{-3}$)	8.0	12.	8.0	6.2
^{13}C ($\times10^{-3}$)	2.8	4.0	2.4	2.4
^{14}N ($\times10^{-3}$)	4.3	4.8	4.3	8.4
^{15}N	0.11	0.11	0.07	0.06
^{16}O ($\times10^{-3}$)	1.2	1.1	2.4	2.4
^{17}O ($\times10^{-3}$)	1.1	1.0	59.	67.
^{18}O ($\times10^{-3}$)	7.8	6.7	3.0	1.5
^{18}F ($\times10^{-3}$)	2.5	2.3	0.9	0.6
^{19}F ($\times10^{-5}$)	10.	9.3	4.2	1.5
^{20}Ne	0.08	0.09	0.11	0.12
^{21}Ne ($\times10^{-5}$)	3.6	3.5	3.1	6.2
^{22}Ne ($\times10^{-6}$)	5.0	6.9	4.4	3.1
^{22}Na ($\times10^{-2}$)	3.5	5.1	3.0	2.3
^{23}Na ($\times10^{-2}$)	8.6	6.6	6.0	5.8
^{24}Mg ($\times10^{-3}$)	2.8	1.9	2.1	1.9
^{25}Mg ($\times10^{-2}$)	3.8	2.4	2.5	2.5
^{26}Mg ($\times10^{-2}$)	1.6	1.2	0.2	0.2
^{26}Al ($\times10^{-3}$)	2.8	2.1	2.7	3.0
^{27}Al ($\times10^{-2}$)	2.8	3.4	1.4	1.4
^{28}Si ($\times10^{-2}$)	2.3	3.5	2.7	2.9
^{29}Si ($\times10^{-2}$)	6.3	7.0	19.	18.
^{30}Si ($\times10^{-2}$)	2.3	2.4	3.1	3.8
^{31}P ($\times10^{-2}$)	3.0	3.0	4.3	3.7
^{32}S ($\times10^{-2}$)	2.1	2.8	3.9	4.0
^{33}S ($\times10^{-3}$)	3.4	1.8	2.0	2.2
^{34}S ($\times10^{-3}$)	1.5	1.3	1.3	0.7

Table 5—Continued

Sequence:	P1995C	S1998	I2001	I2005A
^{35}Cl ($\times 10^{-3}$)	0.9	1.0	1.1	0.5
^{36}Ar ($\times 10^{-4}$)	6.1	2.2	1.5	0.7
^{40}Ca ($\times 10^{-5}$)	2.1	2.4	2.4	1.8

[a]All abundances are given as mass fraction and are to be multiplied by the number following the isotopic designation

REFERENCES

Amari, S., et al. 2001, ApJ, 551, 1065

Anders, E.,& Grevesse, N. 1989, Geochimica et Cosmochimica Acta, 53, 197

Angulo, C., et al. 1999, Nucl. Phys. A, 656, 3

Arnett, W. & Truran, J. 1969, ApJ, 157, 339

Bahcall, J. N., & May R. M. 1969, ApJ, 155,501

Bardayan, D. W., et al. 2000, Phys. Rev. C, 62, 055804

Bardayan, D. W., et al. 2002, Phys. Rev. C, 65, 032801(R)

Beaumel, D., et al. 2001, Phys. Lett. B, 514, 226

Caughlan, G R., & Fowler, W. A. 1988, At. Data Nucl. Data Tab., 40, 283

Chafa, A., et al. 2005, Phys. Rev. Lett., 95, 031101

Champagne, A. E. 2004, priv. comm.

Chen, A. A., et al. 2001, Phys. Rev. C, 63, 065807

Couder, M., et al. 2004, Phys. Rev. C, 69, 022801(R)

Cox, J.P., & Giuli, R. T. 1968, Principles of Stellar Structure, (Gordon & Breach, NYC)

Davids, B. 2004, priv. comm.

de Séréville, N., Berthoumieux, E. & Coc, A. 2005, Nucl. Phys. A, 758, 745

Fox, C. et al. 2005, Phys. Rev. C, 71, 055801

Gehrz, R.D., Truran, J.W., Williams, R.E., & Starrfield, S. 1998, PASP, 110, 3 (G1998)

Graboske, H. C., Dewitt, H. E., Grossman, A. S., Cooper, M. S. 1973, ApJ, 181, 457

Hernanz, M., & José, J. 2000, in Cosmic Explosions, Ed. S. S. Holt & W. W. Zhang, AIP Conference Proceedings # 522, p. 339

Hix, W. R., & Thielemann, F. K 1999, Journal of Computational and Applied Mathematics, 109, 321 (HT1999)

Hix, W. R., Smith, M., Mezzacappa, A., & S.Starrfield. 2000, in Cosmic Explosions, a Conference Proceedings, ed. S. Holt & W. W. Zhang (Melville: AIP), 383

Hix, W. R., Smith, M. S., Starrfield, S., Mezzacappa, A., & Smith, D. L. 2003, Nucl. Phys. A, 718, 620

Iliadis, C., et al. 1996, Phys. Rev. C, 53, 475

Iliadis, C., Champagne, A., Jose, J., Starrfield, S., Tupper, P. 2002, ApJ Supp, 142, 105

Iliadis, C., D'Auria, J. M., Starrfield, S., Thompson, W. J., Wiescher, M., 2001, ApJS, 134, 151

Iliadis, C., et al. 2008, in prep.

Itoh, N. et al. 1996, ApJS, 102, 411

José, J. García-Berro, E., Hernanz, M., Gil-Pons, P. 2007, ApJ, 662, L103

José, J. & Hernanz, M. 1998, ApJ, 494, 680

José, J. Hernanz, M., Amari,S., Lodders, K., Zinner, E. 2004, ApJ, 612, 414

Kahabka, P., van den Heuvel, E. P. J. 1997, ARAA, 35, 69

Krautter, J., Ogelman, H., Starrfield, S., Wichmann, R., & Pfeffermann, E. 1996, ApJ, 456, 788.

Lanz, T., et al. 2005, ApJ, 619, 517

Liu, W., et al. 2003, Nucl. Phys. A, 728, 275

MacDonald, J., Fujimoto, M. Y., Truran, J. W 1985, ApJ, 294, 263

Ness, J.-U., et al. 2007, ApJ, 665, 1334

Nittler, L. R., & Hoppe, P. 2005, Minn. AAS meeting, abstract 6.07

Orio, M. 2004, in Compact Binaries in the Galaxy and Beyond, Revista Mexicana de Astronoma y Astrofsica (Serie de Conferencias)20, 182 (astro-ph/0402035)

Parete-Koon, S., Hix, W. R., Smith, M. S., Starrfield, S., Bardayan, D. W., Guidry, M. W., & Mezzacappa, A. 2003, ApJ, 598, 1239

Parpottas, Y., et al. 2004, Phys. Rev. C, 70, 065805

Petz, A., Hauschildt, P., Ness, J.-H., Starrfield, S. 2005, A&A, 431, 321.

Politano, M., Starrfield, S., Truran, J. W., Weiss, A., & Sparks, W. M. 1995, ApJ, 448, 807

Rolfs, C. E., & Rodney, W. S. 1988, Cauldrons in the Cosmos, U. Chicago Press, Chicago

Rowland, C., et al. 2004, ApJ, 615, L37

Runkle, R. C., Champagne, A. E., & Engel, J. 2001, ApJ, 556, 970

Runkle, R. C., et al. 2005, Phys. Rev. Lett., 94, 082503

Salpeter, E. E. 1954, Australian Journal of Physics, 7, 373

Schatzman, E. 1958, White Dwarfs, North-Holland Publishing Co, Amsterdam.

Schwarz, G. J., Shore, S. N., Starrfield, S., Hauschildt, P. H., Della Valle, M., Baron, E. 2001, MNRAS, 320, 103

Shafter, A. 1997, ApJ, 487, 226.

Shore, S. N., Sonneborn, G., Starrfield, S., Hamuy, M., Williams, R. E., Cassatella, A., Drechsel, H. 1991, 370, 193

Starrfield, S. 1979, in White Dwarfs and Variable Degenerate Stars, ed. H. M. Van Horn, Rochester University Press, Rochester, NY, 274

Starrfield, S. 1989, in Classical Novae, ed. M. Bode & A. Evans, Wiley, NY, 39

Starrfield, S. 2001, in Tetons 4: Galactic Structure, Stars and the Interstellar Medium, ASP Conference Series, Vol. 231. ed. C. E. Woodward, M. D. Bicay, and J. M. Shull., San Francisco: ASP, p.466.

Starrfield, S., Iliadis, C., & Hix, W. R. 2008, "Thermonuclear Processes," in Classical Novae Second Edition, ed. M. Bode & A. Evans, Cambridge University Press, p. 77 (S2008).

Starrfield, S.; Iliadis, C.; Hix, W. R.; Timmes, F. X.; Sparks, W. M. 2007, in Tours Symposium on Nuclear Astrophysics VI. AIP Conference Proceedings, 891, pp. 364

Starrfield, S.; Iliadis, C.; Truran, J. W.; Wiescher, M.; Sparks, W. M. 2001, Nuclear Physics A, 688, 110

Starrfield, S., et al. 1991, in Extreme Ultraviolet Astronomy, ed. R. Malina and S. Bowyer, Pergamon: New York, 168

Starrfield, S., Sparks, W. M., Truran, J.W., Wiescher, M.C. 2000, ApJS, 127, 485 (S2000)

Starrfield, S., Timmes, F. X., Hix, W. R., Sion, E. M., Sparks, W. M., Dwyer, S. J. 2004, ApJL, 612, L53

Starrfield, S., Truran, J.W., Wiescher, M.C., & Sparks, W. M. 1998, MNRAS, 296, 502

Tang, X., et al. 2003, Phys. Rev. C, 67, 015804

Tang, X., et al. 2004, Phys. Rev. C, 69, 055807

Thielemann, F.-K., Arnould, M., & Truran, J. W. 1987, in advances in Nuclear Astrophysics, ed. E. Vangioni-Flam, Gif-sur-Yvette, Editions Frontieres, 525

Thielemann, F.-K., Arnould, M., & Truran, J. W. 1988, in Capture Gamma-Ray Spectroscopy, ed. K. Abrahams & P. Van assche, Bristol, IOP, 730

Timmes, F. X., Woosley, S. E., Weaver, Thomas A. 1995, APJS, 98, 617

Trache, L., et al. 2002, Phys. Rev. C, 66, 035801

Vancraeynest, G., et al. 1998, Phys. Rev. C, 57, 2711

Ward, R. A., & Fowler, W. A. 1980, ApJ, 238, 266

Weiss, A., & Truran, J. W. 1990, A&A, 238, 178

Yaron, O., Prialnik, D., Shara, M. M., Kovetz, A. 2005, ApJ, 623, 398

Zinner, E. 1998, AREPS, 26, 147.

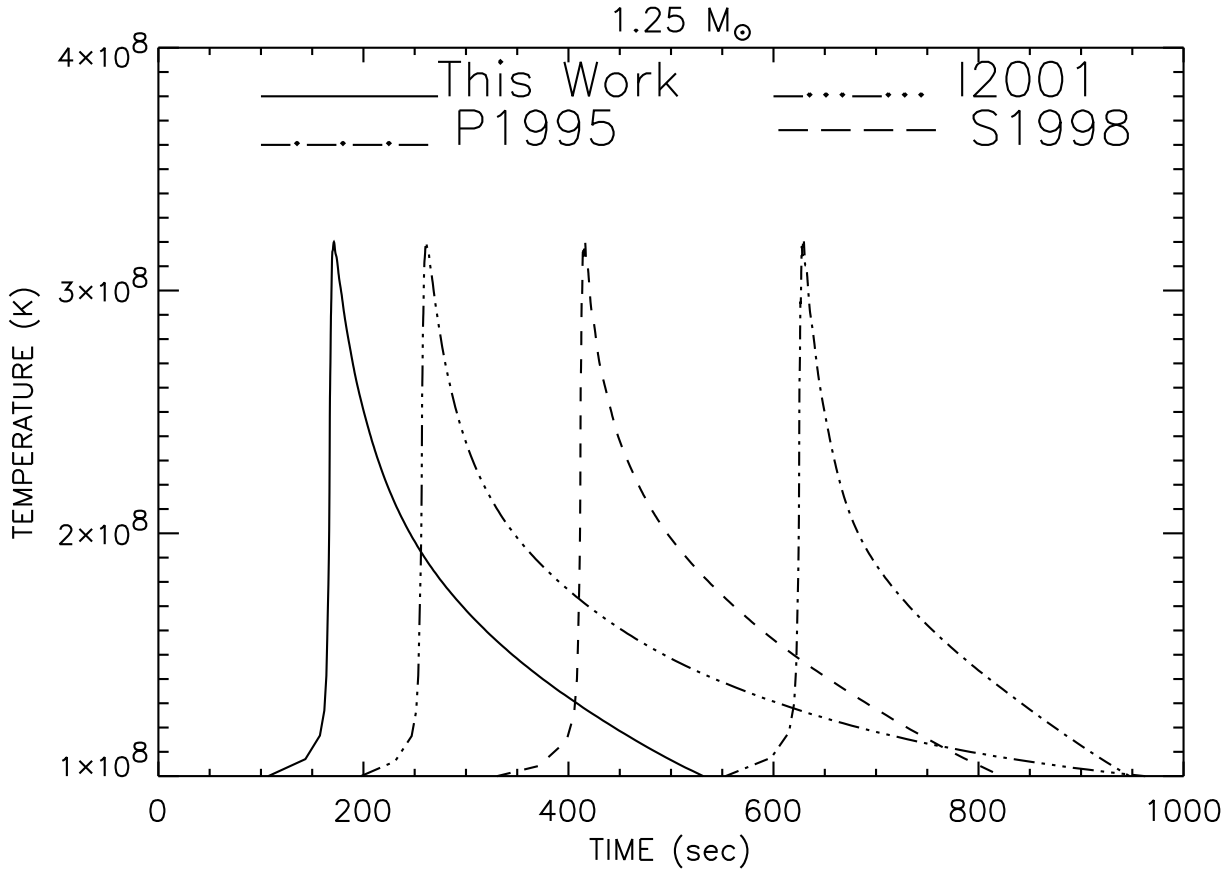

Fig. 1.— The variation with time of the temperature in the zone in which the TNR occurs around the time of peak temperature. For the sequences reported in this paper, this zone is usually one zone above the core-envelope interface. We have plotted the results for four different simulations on a $1.25M_{\odot}$ WD. The identification with calculations done with a specific library is given on the plot. In this plot and all following plots, S1998 refers to Starrfield et al. (1998), P1995 refers to Politano et al. (1995), I2001 refers to Iliadis et al. (2001), and This Work refers to the calculations done with the latest Iliadis reaction rate library (August 2005) and reported in this paper. The details of the associated reaction rate library are given in the text.

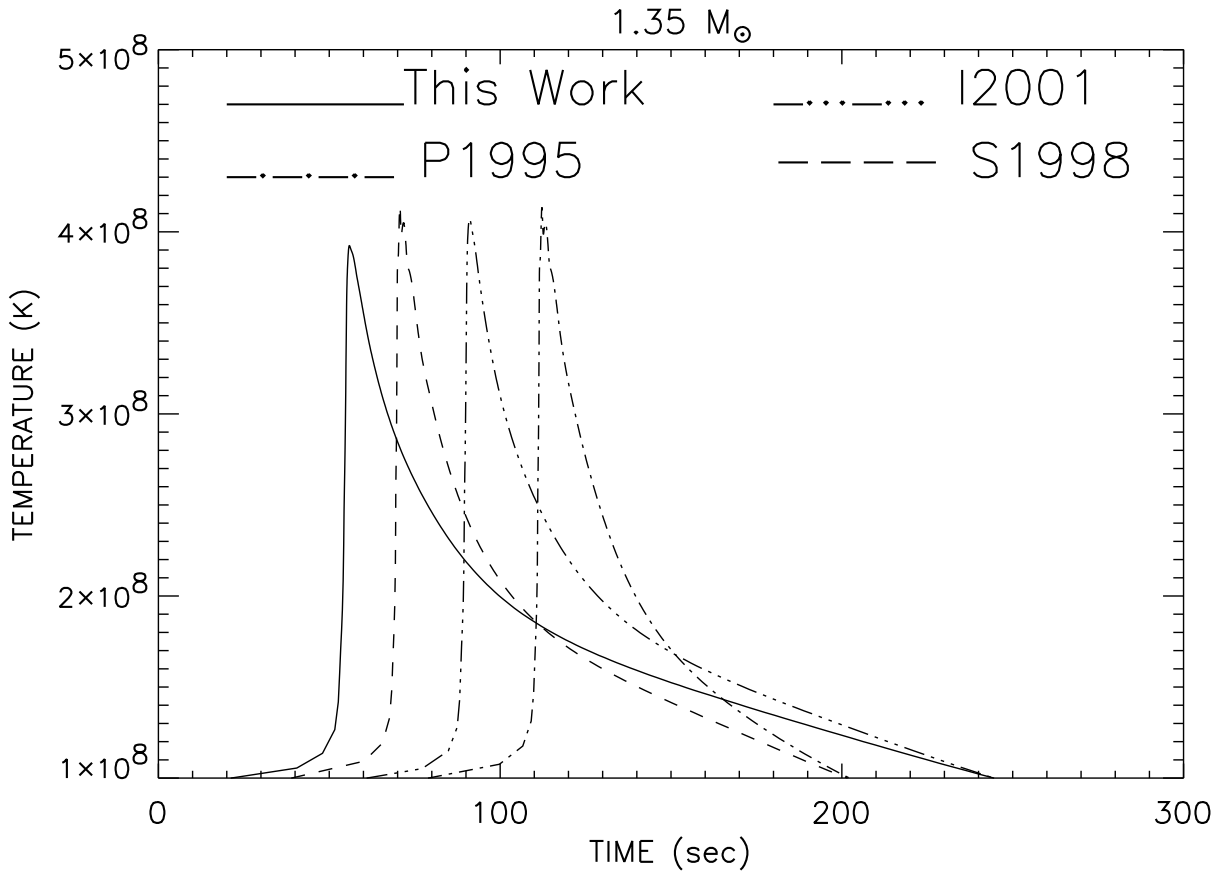

Fig. 2.— Same as for Figure 1 but for a WD mass of $1.35M_{\odot}$.

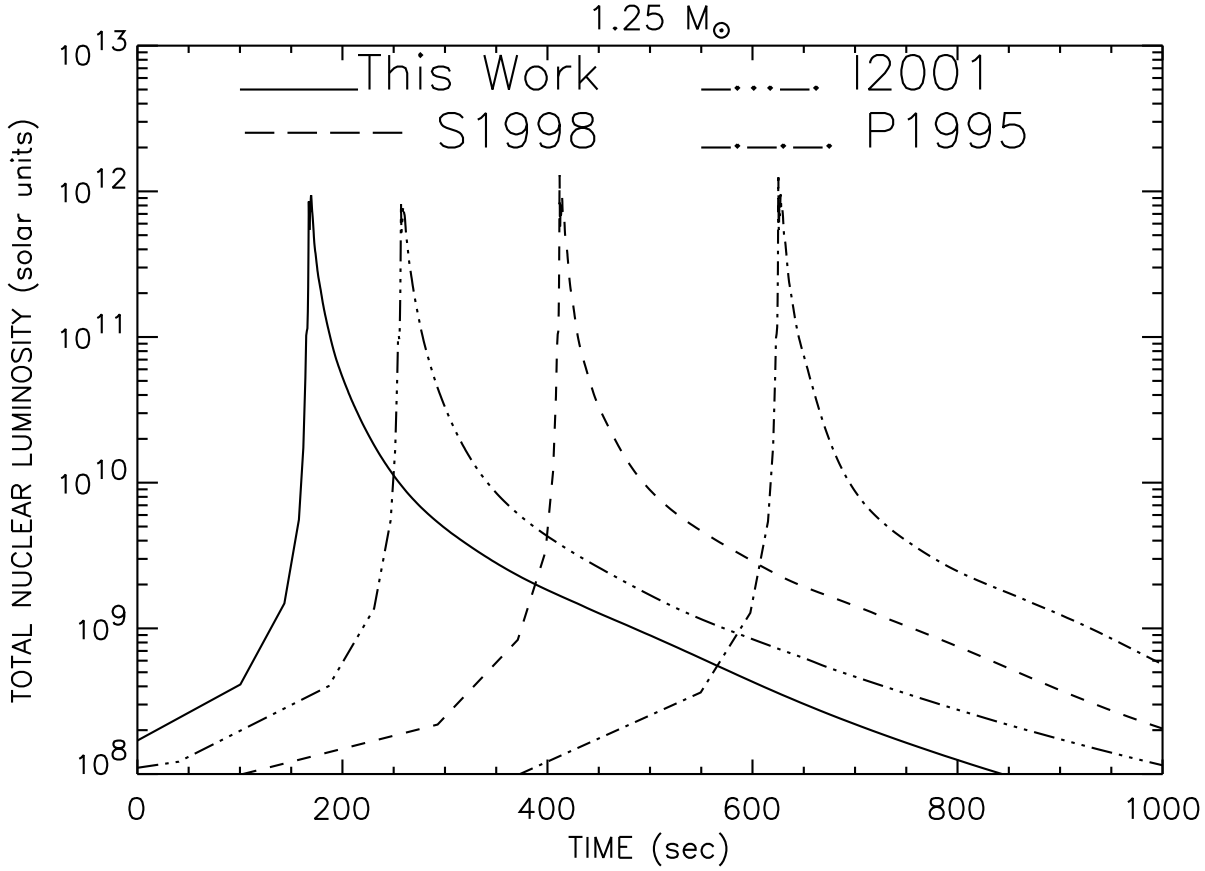

Fig. 3.— The variation with time of the total nuclear luminosity (erg s^{-1}) in solar units ($L_\odot$) around the time of peak temperature during the TNR on a $1.25M_\odot$ WD. We integrated over all zones taking part in the explosion. The identification with each library is given on the plot.

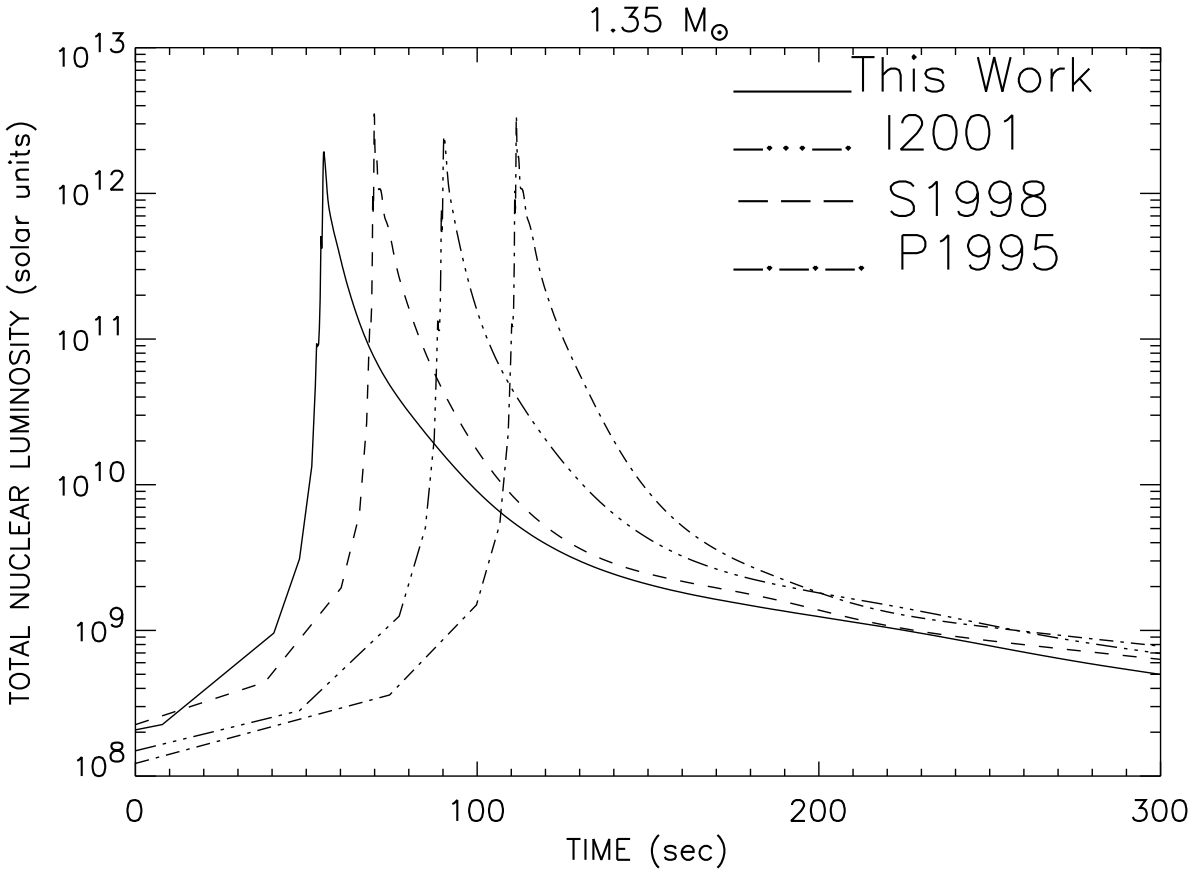

Fig. 4.— Same as for Figure 3 but for a 1.35$M_\odot$ WD.

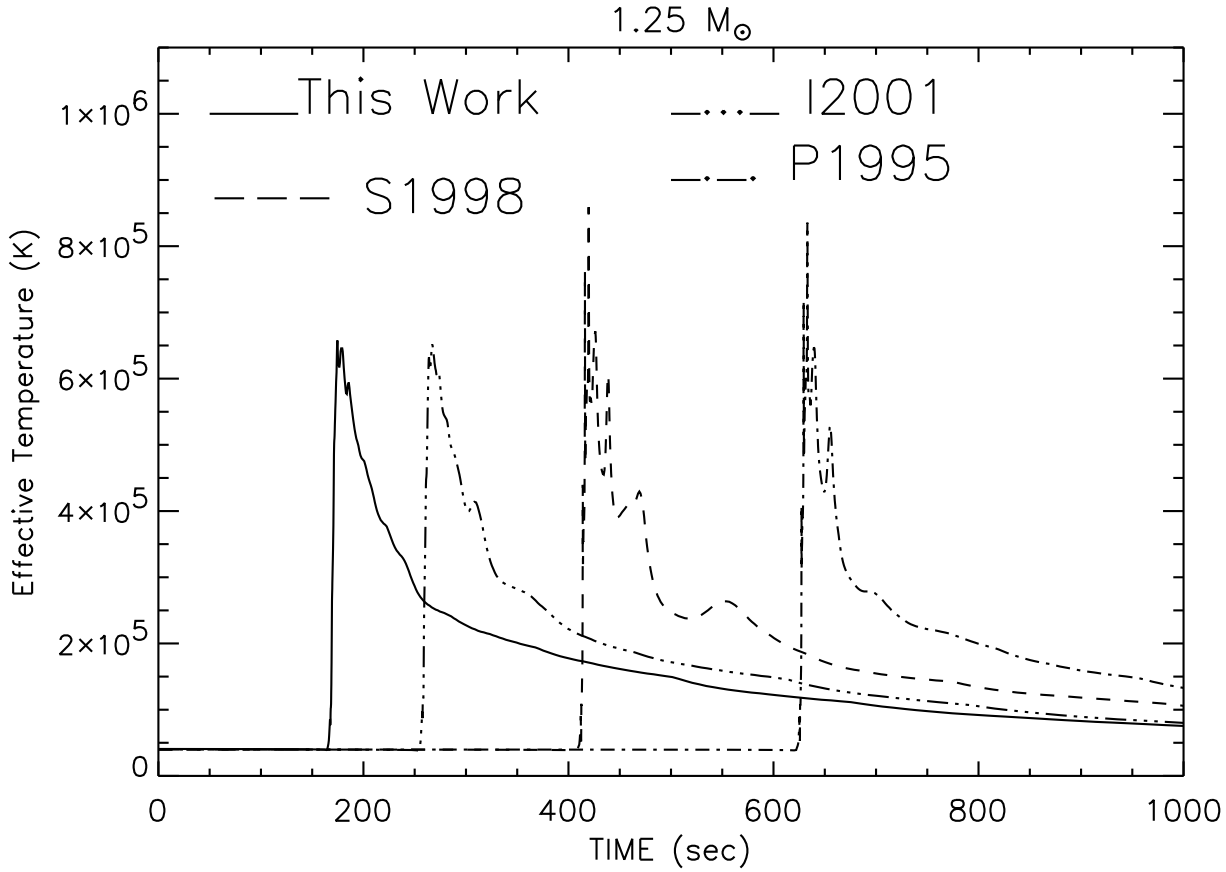

Fig. 5.— The variation with time of the effective temperature around the time when peak temperature is achieved in the TNR for the sequence on the $1.25M_{\odot}$ WD. The time scale is identical to that used in Figure 1 and shows how rapidly the nuclear burning products are transported from the depths of the hydrogen burning shell source to the surface. The different evolutionary sequences are labelled on the plot.

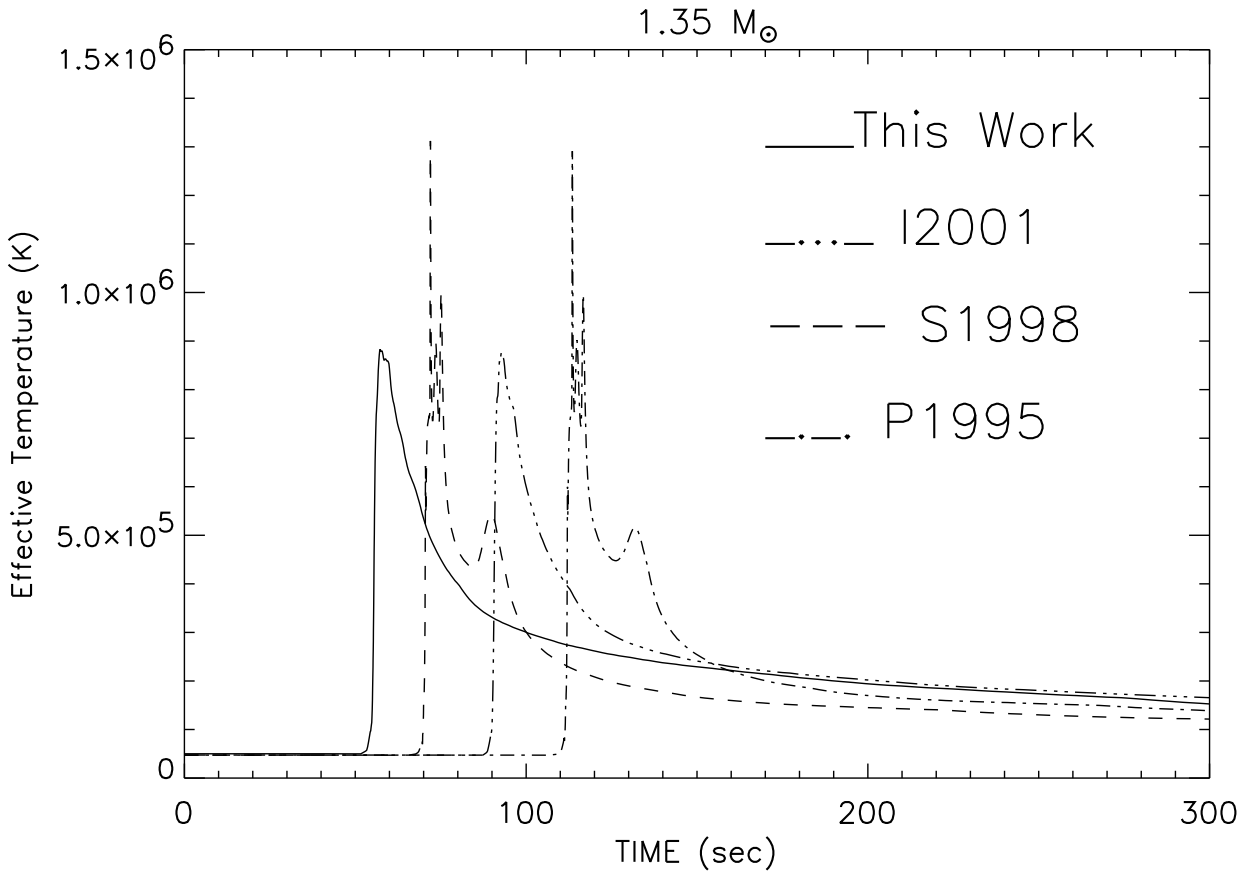

Fig. 6.— Same as for Figure 5 but for a $1.35M_{\odot}$ WD.

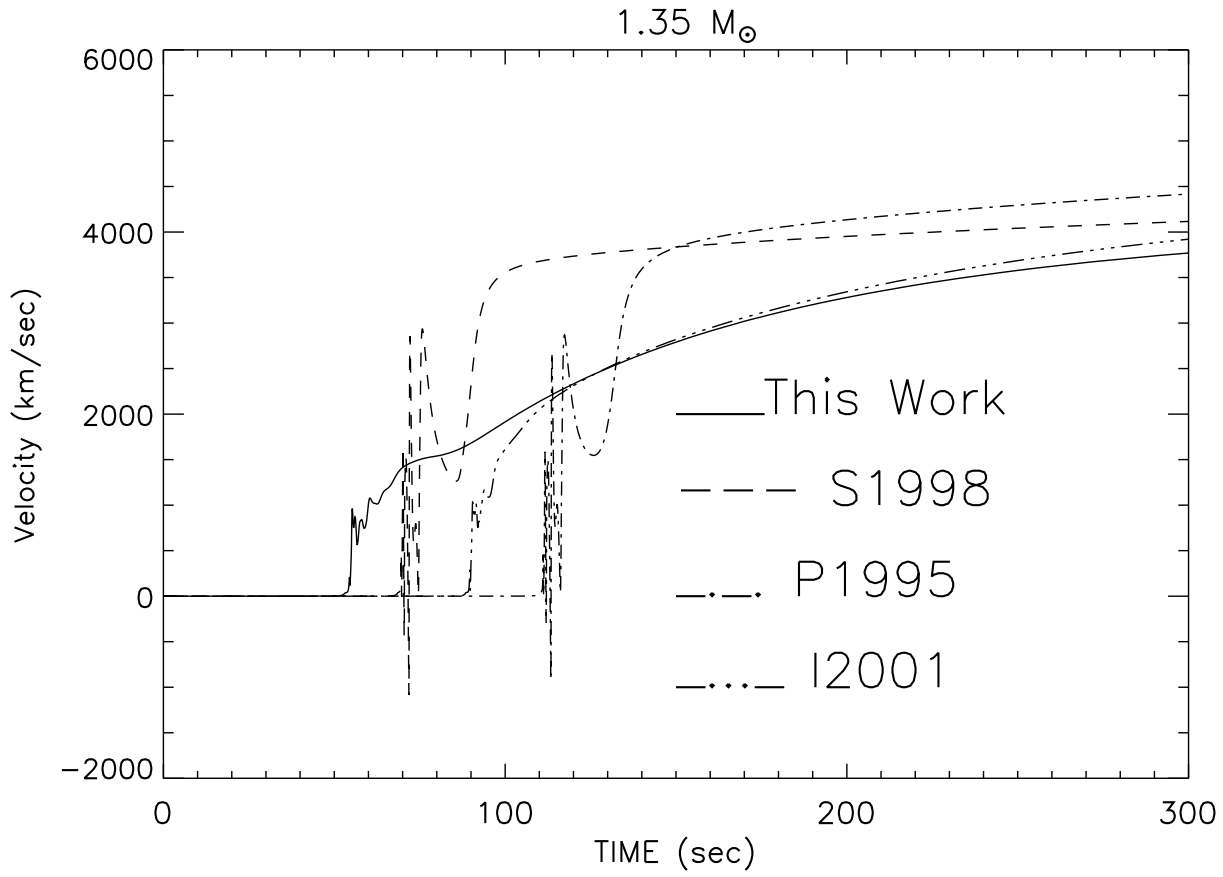

Fig. 7.— The variation with time, over the first 300 sec of the outburst, for the velocity of the surface zone using the four different reaction libraries which are labelled on the plot.

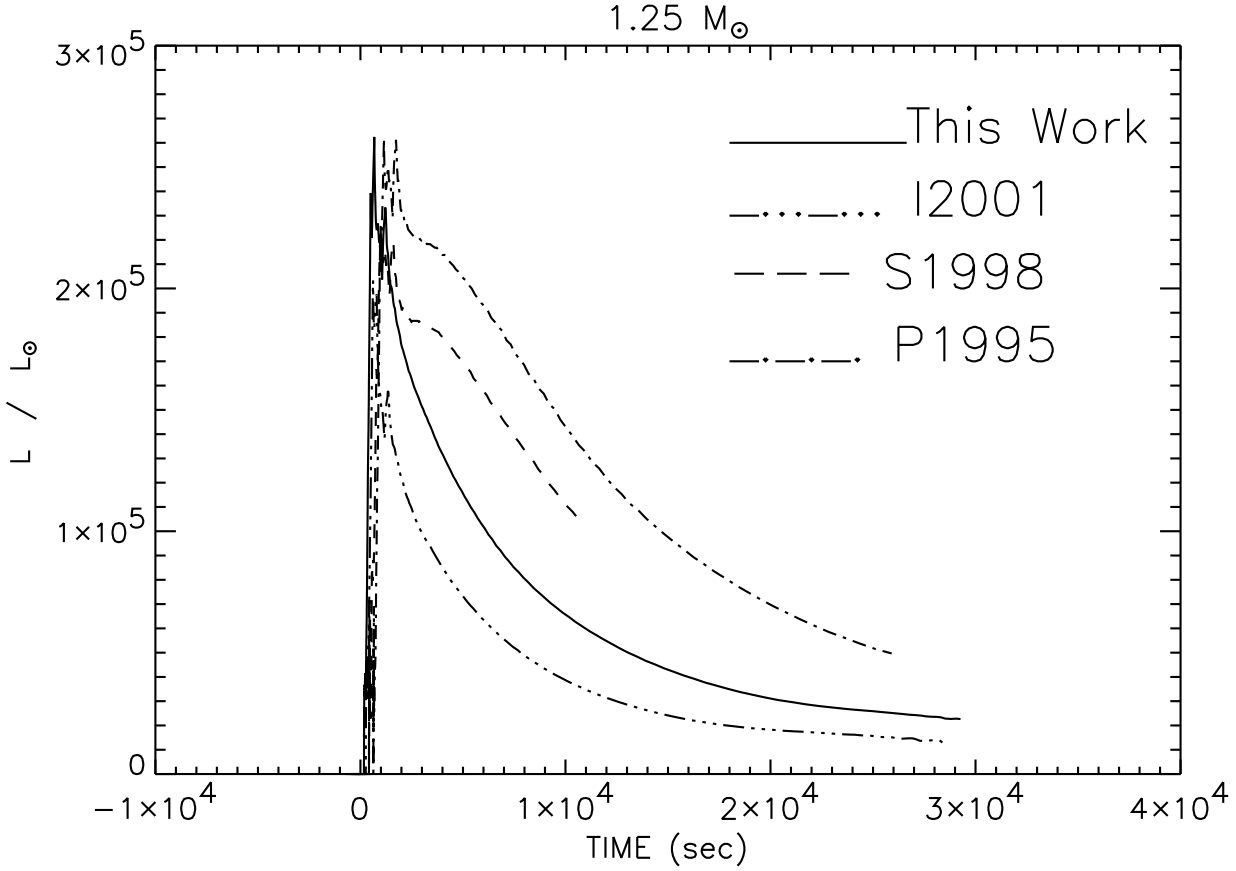

Fig. 8.— The variation in time, over the first 11 hours of the outburst, for the surface luminosity using the four different reaction libraries. The label which identifies each different sequence is given on the plot. Note that as the nuclear physics has improved, the peak luminosity and the luminosity at later times has decreased.

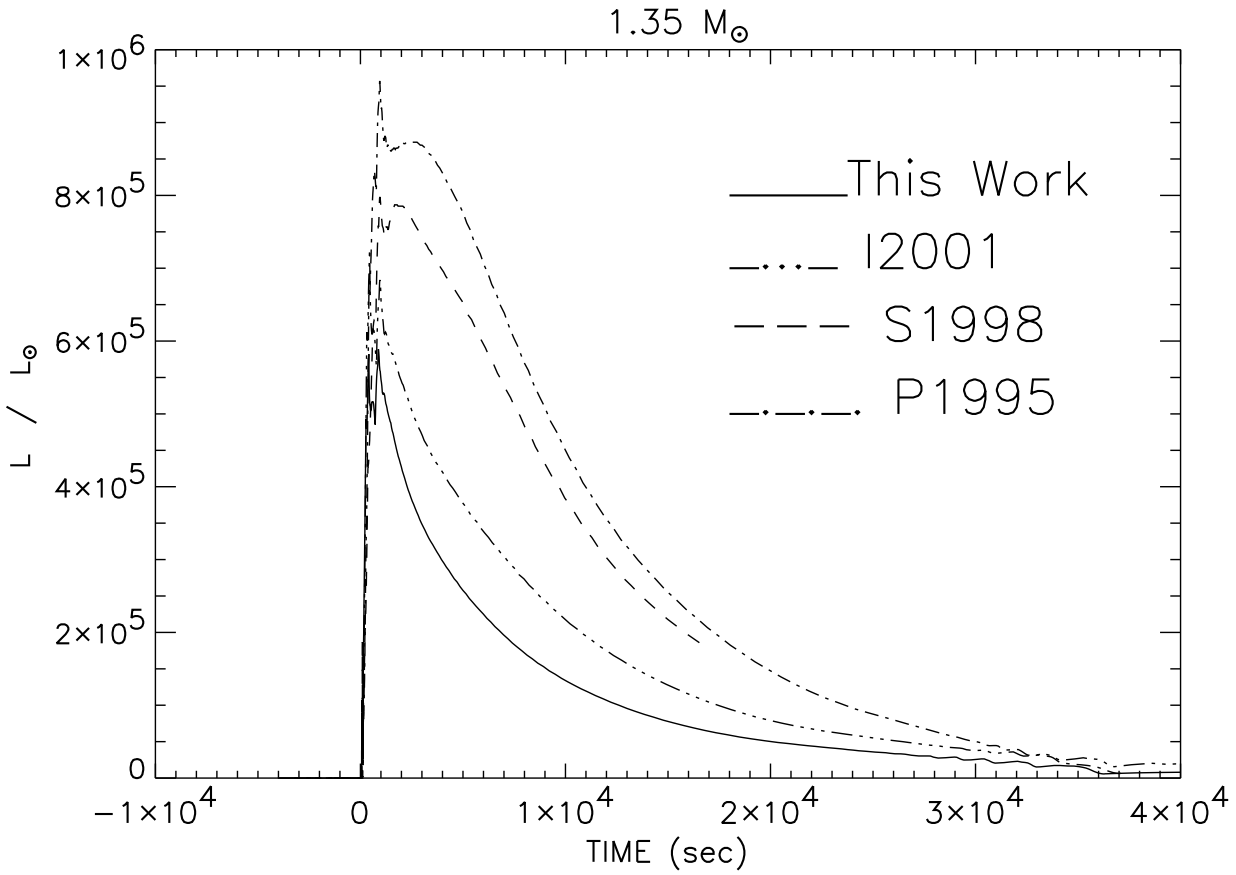

Fig. 9.— Same as for Figure 8 but for a 1.35$M_\odot$ WD.

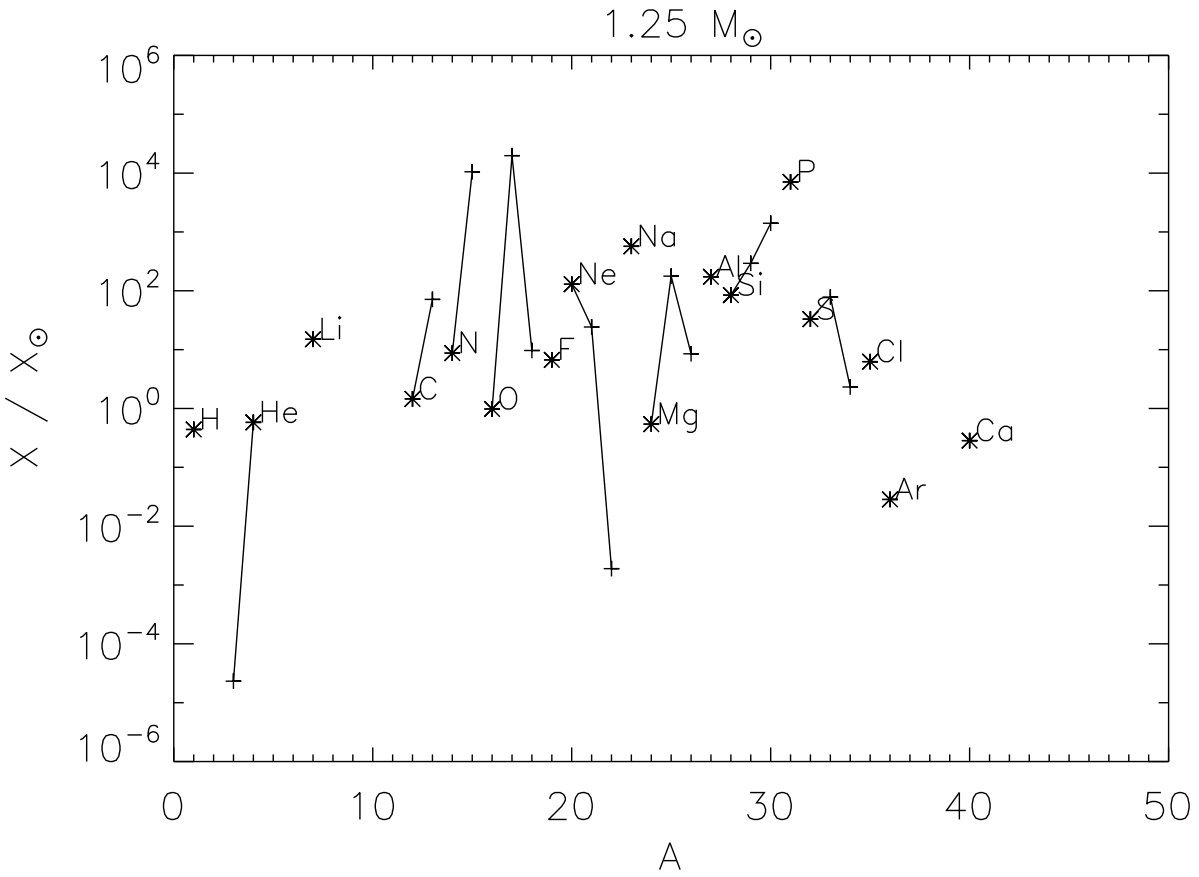

Fig. 10.— The abundances (mass fraction) of the stable isotopes from hydrogen to calcium in the ejected material for the $1.25M_{\odot}$ sequence calculated with the I2005 reaction rate library. The x-axis is the atomic mass and the y-axis is the logarithmic ratio of the abundance divided by the corresponding Anders and Grevesse (1989) Solar abundance. As in Timmes et al. (1995), the most abundant isotope of a given element is designated by an "$*$" and all isotopes of a given element are connected by solid lines. Any isotope above 1.0 is overproduced in the ejecta and a number of isotopes are significantly enriched in the ejecta.

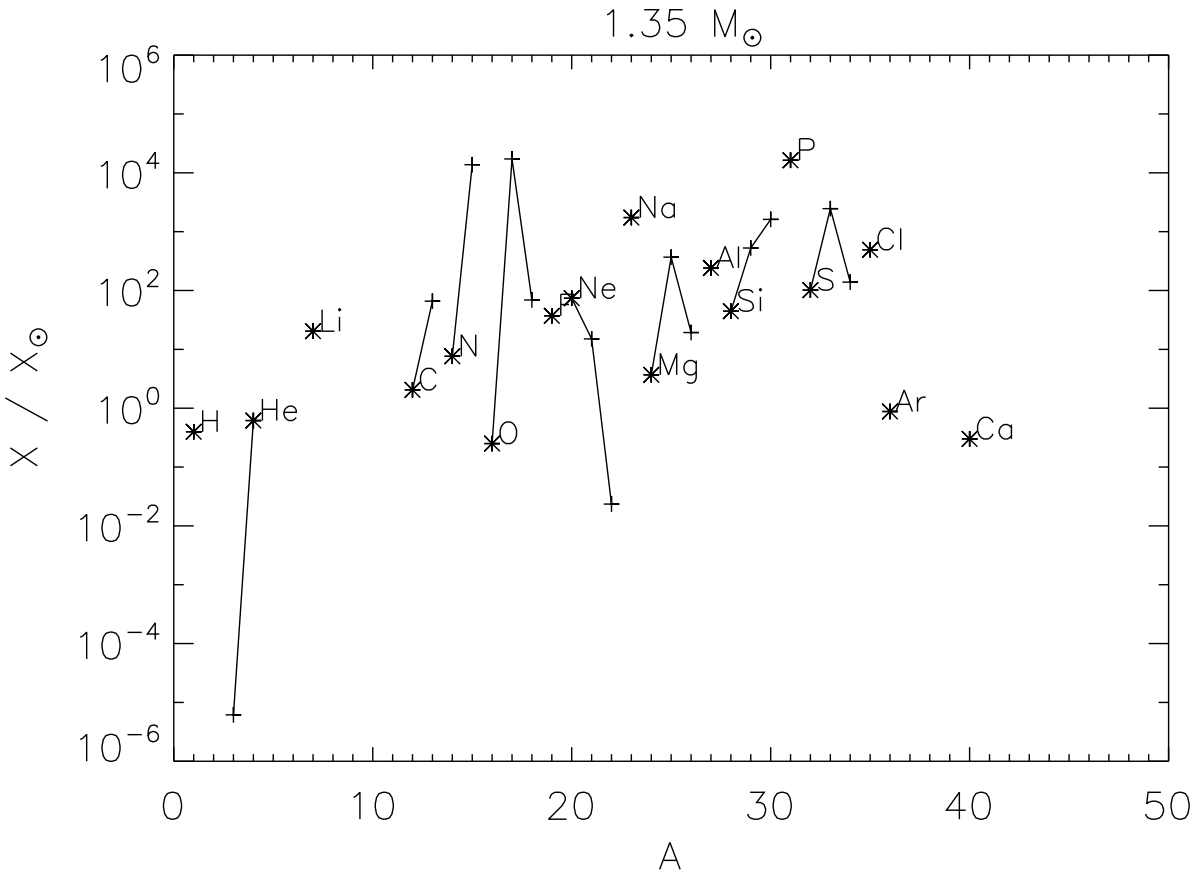

Fig. 11.— Same as for Figure 10 but for a white dwarf mass of $1.35 M_{\odot}$.

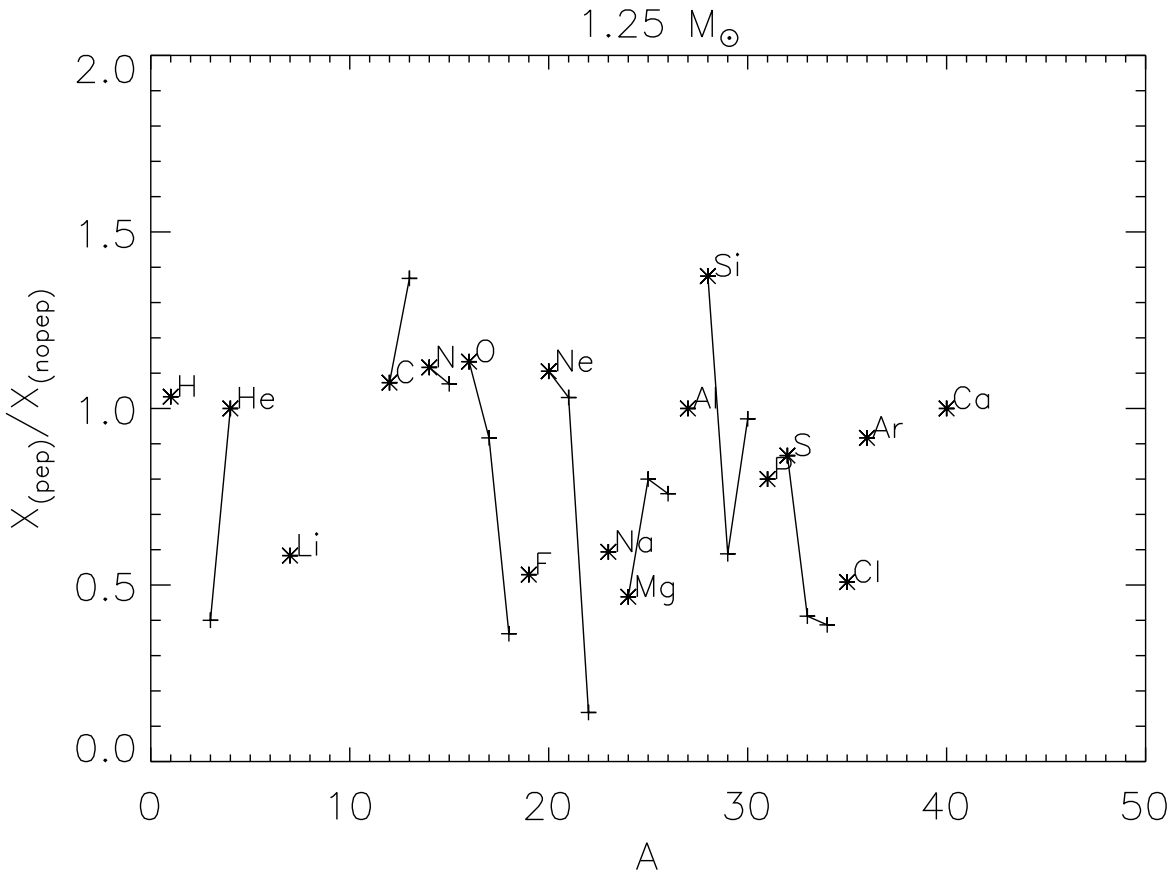

Fig. 12.— The ratio of the abundances of the stable isotopes from hydrogen to calcium in the ejected material for the $1.25M_{\odot}$ sequences calculated with the I2005 reaction rate library. The x-axis is the atomic mass and the y-axis is the linear ratio of the ejecta abundances from the sequence with the *pep* reaction included divided by the corresponding abundance from the sequence calculated without the *pep* reaction included. The most abundant isotope of a given element is designated by an "$*$" and all isotopes of a given element are connected by solid lines.

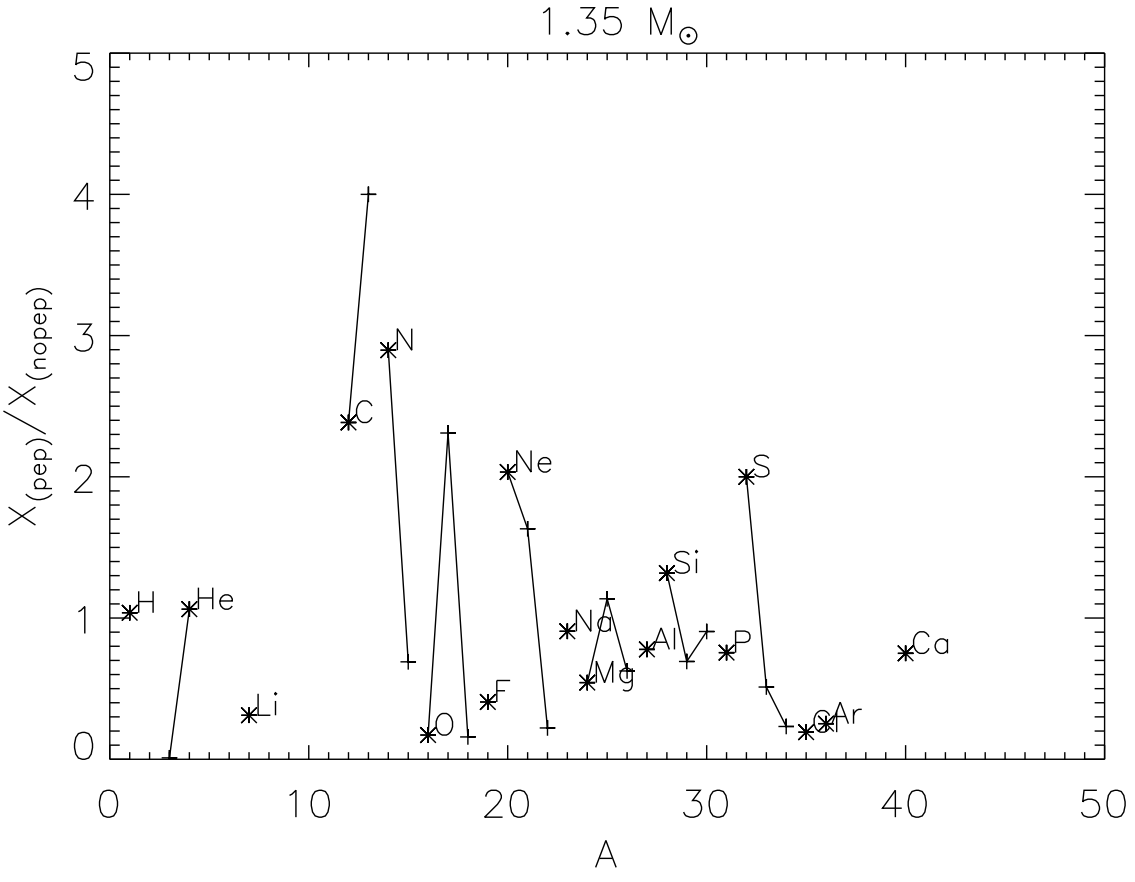

Fig. 13.— Same as for Figure 12 but for a white dwarf mass of $1.35M_{\odot}$.